1
2   **Trends analysis of PM source contributions and chemical tracers in NE Spain during 2004 - 2014: A multi-exponential approach.**

3

4   *Marco Pandolfi [1,*], Andrés Alastuey [1], Noemi Pérez [1], Cristina Reche [1], Iria Castro [1], Victor Shatalov [2] and Xavier Querol[1]*

5   [1] *Institute of Environmental Assessment and Water Research, c/ Jordi-Girona 18-26, 08034 Barcelona, Spain*

6   [2] *Meteorological Synthesizing Centre – East, 2nd Roshchinsky proezd, 8/5, 115419 Moscow, Russia*

7   **Corresponding author: marco.pandolfi@idaea.csic.es*

8

9

10

11 **Abstract**

12 In this work for the first time data from two twin stations (Barcelona, urban background, and Montseny,
13 regional background), located in NE of Spain, were used to study the trends of the concentrations of different
14 chemical species in PM_{10} and $PM_{2.5}$ along with the trends of the PM_{10} source contributions from Positive Matrix
15 Factorization (PMF) model. Eleven years of chemical data (2004–2014) were used for this study. Trends of both
16 specie concentrations and source contributions were studied using the Mann-Kendall test for linear trends and
17 a new approach based on multi-exponential fit of the data. Despite the fact that different PM fractions (PM_1,
18 $PM_{2.5}$, PM_{10}) showed linear decreasing trends at both stations, the contributions of specific sources of pollutants
19 and the related chemical tracers showed exponential (single or double) decreasing trends. The different types
20 of trends observed reflected the different effectiveness and/or time of implementation of the measures taken
21 to reduce the concentrations of atmospheric pollutants (i.e. those implemented in the Industrial Emission
22 Directives and in the Large Combustion Plants Directive). Moreover, the trends of the contributions from
23 specific sources such as those related with industrial activities and with primary energy consumption mirrored
24 the effect of the financial crisis in Spain from 2008. The sources that showed statistically significant downward
25 trends at both Barcelona (BCN) and Montseny (MSY) during 2004-2014 were *Ammonium sulfate*, *Ammonium
26 nitrate*, and *V-Ni bearing* source. The contributions from these sources decreased exponentially during the
27 considered period indicating that the observed decrease was not gradual and consistent over time. Moreover,
28 statistically significant decreasing trends were observed for the contributions to PM from the *Industrial/Traffic*
29 source at MSY (mixed metallurgy and road traffic) and from the *Industrial* (metallurgy mainly) source at BCN.
30 These sources were clearly linked with anthropogenic activities and the observed decreasing trends confirmed
31 the effectiveness of pollution control measures implemented at EU or regional/local levels. The general trends
32 observed for the calculated PMF source contributions well reflected the trends observed for the chemical
33 tracers of these pollutant sources.

34

35   **1. Introduction**

36   Meeting the air quality (AQ) standards is one of the major environmental objectives to protect people from

37   breathing air with high levels of pollution. Many studies have been published in these last years showing clearly

38   that the concentrations of particulate matter (PM), and other air pollutants such as sulphur dioxide (SO_2) and

39   carbon monoxide (CO), have markedly decreased during the last 15 years in many European Countries (EEA,

40   2013; Barmpadimos et al., 2012; Cusack et al., 2012; Querol et al., 2014; Guerreiro et al., 2014 among others).

41   Cusack et al. (2012) reported the reduction in $PM_{2.5}$ concentrations observed at regional background (RB)

42   stations in Spain and across Europe, and, in most cases, the observed reduction was gradual and consistent over

43   time, implying the success of cleaner anthropogenic activities. Barmpadimos et al. (2012) have also shown that

44   PM_{10} concentrations decreased at a number of urban background (UB) and rural background stations in five

45   European countries. Henschel et al. (2013) reported the dramatic decrease in SO_2 levels across six European

46   cities, reflecting the reduction in sulphur content in fuels, as part of EU legislation, coupled with the shift

47   towards the use of cleaner fuels. EEA (2013) also reported general decreases in NO_2 concentrations even if

48   lower compared to PM. However, Henschel et al. (2015) showed that the NO_x concentrations at traffic sites in

49   many EU cities remained unchanged underlining the need of further regulative measures to meet the air quality

50   standards for this pollutant. In fact an important proportion of the European population lives in areas exceeding

51   the AQ standards for the annual limit value of NO_2, the daily limit value of PM_{10} and the health protection

52   objective of O_3 (EEA, 2013; 2015). PM_{10} and NO_2 are still exceeded mostly in urban areas, and especially at

53   traffic sites (Harrison et al., 2008; Williams and Carslaw, 2011; EEA, 2013; among others). In Spain for example it

54   has been reported that more than 90% of the NO_2 exceedances are attributed to road traffic emissions (Querol

55   et al., 2012). Guerreiro et al. (2014) furthermore evidenced notable reduction of ambient air concentration of

56   SO_2, CO and Pb using data available in Airbase (EEA, 2013) and covering 38 European countries. Querol et al.

57   (2014) reported trends for 73 measurement sites across Spain including RB, UB, traffic stations (TS) and

58   Industrial sites (IND). They observed marked downward concentration trends for PM_{10}, $PM_{2.5}$, CO and SO_2 at

59   most of the RB, UB, TR and IND sites considered. Similarly, Salvador et al. (2012) detected a statistically

60   significant downward trends in the concentrations of SO_2, NO_x, CO and $PM_{2.5}$ at most of the urban and urban-

61   background monitoring sites in the Madrid metropolitan area during 1999-2008. Cusack et al. (2012) and Querol

62   et al. (2014) have also shown the highly statistically significant decreasing trends observed at regional level in

63   NE Spain for many trace elements since 2002 (Pb, Cu, Zn, Mn, Cd, As, Sn, V, Ni, Cr).

64   The observed reduction of air pollutants across Europe is the results of efficient emission abatement strategies

65   as for example those implemented in the Industrial Emission Directives (IPPC Integrated Pollution Prevention

66   and Control and subsequent Industrial Emission Directives 1996/61/EC and 2008/1/EC), the Large Combustion

67   Plants Directive (LCPD; 2001/80/EC), the EURO standards on road traffic emission (1998/69/EC, 2002/80/EC,

68   2007/715/EC), the IMO (International Maritime Organization) directive on sulphur content in fuel, and SO_x and

69   NO_x emissions from ships (IMO, 2011; Directive 2005/33/EC). Additionally, the financial crisis, causing mainly a

Atmospheric
Chemistry
and Physics
Discussions

70 reduction of the primary energy consumption from 2008-2009, contributed to the decrease of the ambient

71 concentration of pollutants observed in Spain (Querol et al., 2014).

72 Moreover, national and regional measures for AQ have been taken in many European Countries. In Spain a

73 national AQ plan was approved in 2011 and updated in 2013 by the Council of Ministers of the Government of

74 Spain. Furthermore, 45 regional and 3 local (city scale) AQ plans have been implemented since 2004 in Spain.

75 These AQ Plans mostly focused on improving AQ at major city centers or specific industrial areas.

76 For the aforementioned reasons, it is especially attractive the feasibility of studying the trends of the

77 contributions to PM mass from specific pollutant sources along with the trends of the chemical tracers of these

78 sources.

79 A repository of previous works studying the trends of atmospheric pollutants is reported in the Wikipedia of *The*

80 *Task Force on Measurements and Modelling* (TFMM; https://wiki.met.no/emep/emep-

81 experts/tfmmtrendpublis). The TFMM together with the *Task Force on Emission Inventories and Projections*

82 (TFEIP), the *Task Force on Integrated Assessment Modelling* (TFIAM), and *Task Force on Hemispheric Transport*

83 *of Air Pollution* (TFHTAP) provide a fora for discussion and scientific exchange in support of the EMEP (*European*

84 *Monitoring and Evaluation Programme*; http://www.emep.int/) work plan which is a scientifically based and

85 policy driven programme under the *Convention on Long-range Transboundary Air Pollution* (CLRTAP;

86 http://www.unece.org/env/lrtap/lrtap_h1.html) promoting the international co-operation to solve

87 transboundary air pollution problems. The TFMM was established in 2000 to evaluate measurements and

88 modeling and to further develop working methods and tools. In this contest, five EMEP Centers are undertaking

89 efforts in support of the EMEP work plan, namely the *Centre on Emission Inventories and Projections* (CEIP;

90 http://www.ceip.at/), the *Chemical Coordinating Centre* (CCC; http://www.nilu.no/projects/ccc/), the

91 *Meteorological Synthesizing Centre – West* (MSC-W; http://emep.int/mscw/index_mscw.html), the

92 *Meteorological Synthesizing Centre – East* (MSC-E; http://www.msceast.org/), and the *Centre for Integrated*

93 *Assessment Modelling* (CIAM; http://www.iiasa.ac.at/~rains/ciam.html). In 2014, the TFMM initiated a

94 dedicated exercise to assess the efficiency of air pollution mitigation strategies over the past 20 years to assess

95 the benefit of the CLRTAP main policy instrument. Within this exercise a software was made available by

96 EMEP/MSC-E Center aiming at studying non-linear trends and specifically using multi-exponential fits

97 (https://wiki.met.no/emep/emep-experts/tfmmtrendmethods).

98 For what we are concerned in the majority of studies dealing with trend analysis, linear fits were applied for

99 example by using Mann-Kendall or Theil-Sen methods (Theil, 1950; Sen, 1968), the latter being available for

100 example in the Openair software (Carslaw, 2012; Carslaw and Ropkins, 2012). However, linear fit of data does

101 not always properly represent the observed trends. As we will show, different abatement strategies and periods

102 of implementation may change from one pollutant to another thus leading to different trends for different

103 pollutants, even over the same period. Thus, non-linear fit of the data may be at times strongly recommended.

Atmospheric
Chemistry
and Physics
Discussions

Open Access

EGU

104   In this work we studied the trends of source contributions to PM_{10} and specific chemical species in both PM_{10}

105   and $PM_{2.5}$ using both the consensus methodology (Mann-Kendall) and the multi-exponential approach. PM

106   chemical speciated data collected from 2004 to 2014 at regional (Montseny; NE Spain) and urban (Barcelona,

107   NE Spain) sites were used with this aim. The selected period allowed for trend analysis at these twin stations

108   over a common period. The Positive Matrix Factorization (PMF) model was used to apportion ambient PM_{10}

109   concentrations into pollutant sources. The PMF model, as other Receptor Models (RM), is widely used being a

110   powerful tool to help policy makers to design more targeted approaches to protecting public health. Thus, the

111   novelty of this study lies mainly in a) the opportunity to study the trends of source contributions from PMF

112   model at two twin stations representative of the urban and regional environments in the Western

113   Mediterranean, and, b) in the use of a novel non-linear approach for trend studies.

114

115   **2. Measurement sites and Methodology**

116   **2.1 Measurement sites**

117   The Montseny measurement station (MSY, 41°46'45.63" N, 02°21'28.92" E, 720 m a.s.l.) is a regional

118   background site in NE of Spain (Figure 1). The MSY station is located within a regional natural park about 50 km

119   to the NNE of the city of Barcelona (BCN) and 25 km from the Mediterranean coast. This site is representative of

120   the typical regional background conditions of the Western Mediterranean Basin (WMB) characterized by severe

121   pollution episodes affecting not only the coastal sites closest to the emission sources, but also the more

122   elevated rural and remote areas land inwards due to thermally driven winds (i.e. Pérez et al., 2008; Pey et al.,

123   2010; Pandolfi et al., 2011; 2014). This station is part of ACTRIS (www.actris.net) and GAW (www.wmo.int/gaw)

124   networks, EMEP (http://www.emep.int/) and the measuring network of the Government of Catalonia.

125   The Barcelona measurement station (BCN, 41°23'24.01" N, 02°06'58.06" E, 68 m a.s.l.) is an urban background

126   measurement site influenced by vehicular emissions from one of the main avenues of the city (Diagonal

127   Avenue) located at a distance of around 300 m (cf. Fig. 1). The BCN measurement site is part of the Air Quality

128   measuring network of the Government of Catalonia. The Metropolitan Area of Barcelona (BMA), with nearly 4.5

129   million inhabitants, covers an 8 km wide strip between the Mediterranean Sea and the coastal mountain range.

130   Several industrial zones, power plants, and highways are located in the area, making this region to one of the

131   most polluted in the WMB (i.e. Querol et al., 2008; Amato et al., 2009; Pandolfi et al., 2012; 2013; 2014). At BCN

132   the location of the measuring station changed in 2009 when it was moved by around 500 m (cf. Fig. 1). The

133   effect of this change on PM measurements performed at BCN will discuss later.

134

135

136

Atmospheric
Chemistry
and Physics
Discussions

137 **2.2 Real-time and gravimetric PM measurements**

138 Real-time PM concentrations were continuously measured at 1h resolution by optical particle counters (OPC)

139 using GRIMM spectrometers (GRIMM 180 at MSY, and GRIMM 1107, 1129 and 180 at BCN). Hourly PM

140 concentrations were corrected by comparison with 24h gravimetric mass measurements of PM_x (Alastuey et al.,

141 2011).

142 For gravimetric measurements 24h PMx samples were collected at both stations every 3-4 days on 150 mm

143 quartz micro-fiber filters (Pallflex QAT and Whatman) with a high-volume (Hi-Vol) samplers (DIGITEL DH80

144 and/or MCV CAV-A/MSb at 30 m^3h^{-1}). The mass of PM_{10} and $PM_{2.5}$ samples collected on filters was determined

145 using the EN 12341 and the EN14907 gravimetric procedures, respectively.

146

147 **2.2.1 PM chemical speciated data**

148 Once the gravimetric mass was determined from filters, the samples were analyzed with different techniques

149 including acidic digestion (½ of each filter; HNO_3:HF:$HClO_4$), water extraction of soluble anions (¼ of each filter),

150 and thermal-optical analysis (1.5 cm^2 sections). Inductively Coupled Atomic Emission Spectrometry, ICP-AES,

151 (IRIS Advantage TJA Solutions, THERMO) was used for the determination of the major elements (Al, Ca, Fe, K,

152 Na, Mg, S, Ti, P), and Inductively Coupled Plasma Mass Spectrometry, ICP-MS, (X Series II, THERMO) for the

153 trace elements (Li, Ti, V, Cr, Mn, Co, Ni, Cu, Zn, As, Se, Rb, Sr, Cd, Sn, Sb, Ba, rare earths, Pb, Bi, Th, U). Ionic

154 Chromatography was used for the concentrations of NO_3^-, SO_4^{2-} and Cl^-, whereas NH_4^+ was determined using a

155 specific electrode MODEL 710 A+, THERMO Orion. The levels of OC and EC were determined by a thermal-

156 optical carbon analyzer (SUNSET), using protocol EUSAAR_2. Other analytical details may be found in Querol et

157 al. (2009).

158 Following the above procedures, PM_{10} and $PM_{2.5}$ chemical speciated data were obtained at MSY for the period

159 2004-2014 resulting in 1093 and 794 samples, respectively. At BCN PM_{10} and $PM_{2.5}$ data were obtained during

160 2004-2014 resulting in 1037 and 1063 samples, respectively.

161

162 **2.3 Positive Matrix Factorization (PMF) model.**

163 The PMF model (PMFv5.0, EPA) was used on the collected daily speciated data for source identification and

164 apportionment in PM_{10} at both sites. Detailed information about the PMF model can be found in literature

165 (Paatero and Tapper 1994; Paatero 1997; Paatero and Hopke 2003; Paatero et al. 2005). The PMF model is a

166 factor analytical tool reducing the dimension of the input matrix in a limited number of factors (or sources) and

167 it is based on the weighted least-squares method. Thus, most important in PMF applications is the estimation of

168 uncertainties of the chemical species included in the input matrix. In the present study, individual uncertainties

Atmospheric
Chemistry
and Physics
Discussions

Open Access

169 and detection limits were calculated as in Escrig et al. (2009) and Amato et al. (2009). Thus, both the analytical

170 uncertainties and the standard deviations of species concentrations in the blank filters were considered in the

171 uncertainties calculations. The signal-to-noise ratio (S/N) was estimated starting from the calculated

172 uncertainties and used as a criteria (S/N >2) for selecting the species used within the PMF model. In order to

173 avoid any bias in the PMF results, the data matrix was uncensored (End user's guide to multilinear engine

174 applications from Pentti Paatero). The PMF was run in robust mode (Paatero 1997), and rotational ambiguity

175 was handled by means of the F_{PEAK} parameter (Paatero et al. 2005). The optimal number of sources was selected

176 by inspecting the variation of the objective function Q (defined as the ratio between residuals and errors in each

177 data value) with varying number of sources (i.e. Paatero et al., 2002) and by studying the physical

178 meaningfulness of the calculated factors.

179 **2.4 Mann-Kendall (MK) fit**

180 The purpose of the Mann-Kendall (MK) test (Mann 1945, Kendall 1975, Gilbert 1987) is to statistically assess if

181 there is a monotonic upward or downward trend of the variable of interest over time. A monotonic upward

182 (downward) trend means that the variable consistently increases (decreases) through time.

183

184 **2.5 Multi-exponential (ME) fit**

185 A Program aiming at studying trends of time series of air pollution in the multi-exponential form was developed

186 within the TFMM by MSC-E group (Shatalov et al., 2015). Annual, monthly and daily resolution data can be

187 analyzed with the help of this program. Since in this paper we will apply the program to annual averages of

188 specie concentrations and source contributions, we restrict the description of the multi-exponential

189 approximations for this case. In particular, seasonal variations are not included into consideration. The basic

190 equations solved by the program for this particular case (annual averages) are reported below:

191

192 $$C_t = a_1 \cdot \exp\left(-\frac{t}{\tau_1}\right) + a_2 \cdot \exp\left(-\frac{t}{\tau_2}\right) + \ldots + a_n \cdot \exp\left(-\frac{t}{\tau_n}\right) + \omega_t \quad (1)$$

193

194 Where, C_t are the values of the considered time series, with t = 1, …, N, N being the length of the series (years),

195 τ_n are the characteristic times of the considered exponential, and a_n are constants. In the case of single

196 exponential decay (n=1) the characteristic time τ is the time at which the pollutant concentration is reduced to

197 1/e (= 0.3678) times its initial value. Both τ_n and a_n are calculated by the program by means of the least square

198 method minimizing the residue ω. The number of exponential terms that should be included into the

199 approximation can be evaluated using F-statistics (i.e. Smith, 2002). For example, the *F*-statistics for the

200 evaluation of the statistical significance of the second term in equation (1) for n = 2 can be calculated as:

Atmospheric
Chemistry
and Physics

Discussions

Open Access

EGU

201

202 $$F = \frac{(SS_1 - SS_2)}{2 \cdot s}$$ (2)

203

204 where SS_1 and SS_2 are sums of squares of residual component for approximations with one and two exponential

205 terms, respectively, and s is the estimate of standard deviation of residual component. This statistics follows

206 approximately the Fisher distribution with 2 and $N - 2$ degrees of freedom. Second exponential is considered to

207 be significant if F exceeds the corresponding threshold value at the chosen significance level.

208 The following parameters can be calculated from equation (1):

209   - Total Reduction (TR): $TR = \frac{(C_{beg} - C_{end})}{C_{beg}} = 1 - \frac{C_{end}}{C_{beg}}$ (3)

210   - Annual reduction for year i: $R_i = \frac{\Delta C_i}{C_i} = 1 - \frac{C_{i+1}}{C_i}$ (4)

211   - Average annual reduction: $R_{av} = 1 - \left(\frac{C_{end}}{C_{beg}}\right)^{\frac{1}{N-1}}$ (5)

212 The formula for calculation of average annual reduction takes into account that the ratio C_i+1 / C_i is a

213 multiplicative quantity, so that geometrical mean of ratios should be used.

214 The MSC-E also proposed a statistic which can be used to check if the trends are linear or not (Non-Linearity:

215 NL). More detailed description of the multi-exponential approach is available in the TFMM wiki and in the MSC-

216 E Technical report 2015 (Shatalov et al., 2015).

217

218 **3. Results**

219 Results will be presented and discussed in the following order: First (*Paragraph 3.1*), we will compare the trends

220 at both stations of PM$_x$ concentrations from optical counters (OPC; annual data coverage around 90%) and from

221 24h gravimetric samples (filters; annual data coverage around 20-30%). This comparison will demonstrate the

222 feasibility of studying trends of pollutant concentrations from filters analyses despite the relatively low annual

223 data coverage. Second (*Paragraph 3.2*), we will compare the magnitude of the trend of PM$_{2.5}$ concentrations at

224 MSY during 2004-2014 (period selected for this study) with the magnitude of trends calculated at the same

225 station over different periods, namely 2002-2010 (the period used in Cusack et al., 2012) and 2002-2014

226 (representing the largest period of gravimetric PM$_{2.5}$ measurements available so far at MSY station). This

227 comparison was performed in order to study the effects of meteorology on the magnitude of the trends over

228 relatively short periods. The gravimetric concentrations of PM$_{2.5}$ were used with this aim. Third, we will present

229 and discuss the trends at both stations of chemical species in both PM$_{10}$ and PM$_{2.5}$ from 24h filter analyses

230 (*Paragraph 3.3*). Fourth, we will discuss the sources of pollutants identified by PMF model in PM$_{10}$ at both sites

231 (*Paragraph 4.0*). Finally, we will present and discuss the trends of PM_{10} source contributions at BCN and MSY

232 (*Paragraph 4.1*). In *Paragraph 4.1* we will provide possible explanations for the observed trends.

233

3.1 Trends of PM: Comparison between gravimetric and real-time optical measurements

235 In this section we evaluate the feasibility of studying the trends of PM concentrations from gravimetric samples

236 by comparing the trends of 24h PM concentrations from filters to those obtained using daily averaged real-time

237 data from optical counters (OPC). In fact, the annual coverage of gravimetric measurements was around 30% at

238 both sites, whereas the OPC measurements had an annual coverage of around 90%. Note that the

239 recommended annual data coverage for trend studies is typically 75%.

240 Table 1 reports the trends (during 2004-2014) of annual mean concentrations of different PM size fractions

241 (from both OPC and gravimetric measurements) at both BCN and MSY calculated using both the Mann-Kendall

242 (MK) and multi-exponential (ME) fits. Gravimetric PM_1 concentrations were not available for the whole period

243 and only OPC data were reported in Table 1. Similarly, calculated PM_x concentrations (PM_{1-10} and $PM_{2.5-10}$) and

244 PM ratios (PM_1/PM_{10} and $PM_{2.5}/PM_{10}$) were reported only for OPC data. Following the MK test, statistically

245 significant decreasing trends were observed for all PM size fractions at BCN (ranging from   -2.18 %/yr with

246 p<0.05 for $PM_{2.5-10}$ to -3.89 %/yr with p<0.001 for $PM_{2.5}$), whereas at Montseny only the $PM_{2.5}$ fraction showed a

247 statistical significant decreasing trend (-1.87 %/yr, p<0.1 from gravimetric measurements). The higher

248 statistically significance of the PM_x trends observed at BCN compared to MSY was likely due to the change of

249 the measuring station in 2009 in BCN (cf. Fig. 1). Based on the comparison between simultaneous PM_x chemical

250 speciated data collected at both BCN measurement sites during 1 month (not shown) we concluded that after

251 2009 the BCN measuring site was less affected by mineral matter and, to a lesser extent, by road traffic

252 emissions both being important sources of PM in Barcelona. In Figure 1 we highlighted the proximity of the BCN

253 measuring station before 2009 to an unpaved parking and different construction works. The effect of the

254 change of the station in BCN in 2009 on PM_{10} gravimetric measurements was reported in Supporting

255 Information (Figure SI-1). Thus, we will discuss here the magnitude of the trends of PM_x concentrations at MSY

256 only. However, despite the change of station, the comparison between BCN and MSY for specific chemical

257 species and pollutant sources not linked with these two pollutant sources (mineral matter and road traffic

258 emissions) was possible.

259 Table 1 shows that the trends of different PM_x size fractions at MSY were linear (L) during the period 2004-

260 2014. In fact the non-linearity parameter (NL), which is an estimation of how much the trend differs from the

261 linear one, was always lower than 10% which was used as threshold for non-linearity (Shatalov et al., 2015). The

262 characteristic times (τ) from ME fit of PM_x reported in Table 1 were not directly comparable between BCN and

263 MSY again because of the change of the station occurred in BCN in 2009. As a consequence the characteristic

264 times (τ) for PM_1, $PM_{2.5}$ and PM_{10} at BCN were much lower than at MSY indicating a steeper decrease of PMx

Atmospheric
Chemistry
and Physics
Discussions

265   concentrations at BCN compared to MSY (cf. Eq. 1 and Figure SI-1 in Supporting Information). Moreover, much

266   higher NL and total reductions (TR) were obtained at BCN compared to MSY.

267   Following the MK test, at MSY station the PM_1 fraction from OPC showed non-statistically significant decreasing

268   trend (-1.25 %/yr), whereas for the PM_{10} fraction (OPC) no trend was observed (0.0 %/yr). The magnitude of the

269   trends of PM_{10} and $PM_{2.5}$ concentrations at MSY from gravimetric measurements (-0.47 %/yr and -1.87 %/yr,

270   respectively) confirmed what observed using data from OPC (0.00 %/yr and -1.78 %/yr, respectively).

271   Similarities were also observed between OPC and gravimetric measurements of $PM_{2.5}$ and PM_{10} at BCN (cf.

272   Table 1). Thus, despite the different data coverage the magnitudes of the trends calculated from OPC and

273   gravimetric measurements were very similar. We will show later (*Paragraph 4.1*) that despite the fact that the

274   gravimetric concentrations of PM_{10} at MSY only slightly decreased monotonically with time (-0.47 %/yr with

275   p>0.1; cf. Table 1), the contributions from specific PM_{10} pollutant sources from PMF model related with

276   anthropogenic activities showed non-linear (i.e. exponential) statistically significant decreasing trends. For

277   example the *Ammonium sulfate* source contribution to PM_{10} at MSY decreased at the rate of -2.02 %/yr with

278   p<0.05 from MK test and double exponential fit of the data was needed; cf. Table 5). At MSY the PM_{1-10} and

279    $PM_{2.5-10}$ size fractions showed non-statistically significant increasing trends of around 0.9 %/yr and 0.62 %/yr,

280   respectively. The decreasing trends of these two PM size fractions at BCN (-2.34 %/yr and -2.18 %/yr for PM_{1-10}

281   and $PM_{2.5-10}$, respectively) were statistically significant however, as already noted, these decreases were largely

282   explained by the change of the BCN measuring station in 2009. Moreover, at MSY non significant decreasing

283   trends were observed for the ratio PM_1/PM_{10}, with magnitude of -1.25 %/yr and for the ratio $PM_{2.5/10}$ decreasing

284   at the rate of -0.62 %/yr. At MSY, on average, the residual component (RC) was quite low and around 8-26% for

285   all PM fractions. Total reductions at MSY (TR) ranged from 8-12% for PM_{10} (not statistically significant) to 24%

286   for $PM_{2.5}$ (statistically significant at p<0.1).

287

3.2 Trends of PM: Comparison among different periods

289   In this section we compared the magnitude of the trends of gravimetric $PM_{2.5}$ concentrations at MSY over

290   different periods (2002-2010; 2004-2014 and 2002-2014) in order to evaluate the effects of meteorology-driven

291   interannual variability on PM concentrations and trends. Note that the period 2004-2014 was the period chosen

292   for trends analysis in this study given that gravimetric $PM_{2.5}$ measurements at BCN were available since 2004.

293   Conversely, at MSY $PM_{2.5}$ gravimetric measurements started in 2002. Figure 2 shows the trends of $PM_{2.5}$

294   concentrations at MSY calculated using both MK (Fig. 2a) and ME (Fig. 2b) fits for the three different periods.

295   The period 2002-2010 was the period considered in the paper from Cusack et al. (2012) presenting the trends of

296    $PM_{2.5}$ gravimetric mass and chemical species in $PM_{2.5}$ at MSY. The period 2002-2014 is the largest period

297   available so far at MSY with $PM_{2.5}$ filter measurements. The trend observed at MSY for the $PM_{2.5}$ fraction during

298   2004-2014 confirmed what already observed by Cusack et al. (2012) at the same station for the period 2002 –

299   2010. In Cusack et al. (2012) the MK test provided a decreasing trend of around -3.4 %/yr at 0.01 significance

Atmospheric
Chemistry
and Physics
Discussions

300   level during 2002 – 2010. Considering the period 2004 – 2014, a decreasing trend of -1.87 %/yr at 0.1

301   significance level was observed. Thus, a statistically significant trend for $PM_{2.5}$ at regional level can be confirmed

302   even considering different periods. However, the difference observed in the magnitude of the trends during

303   2004-2014 compared to the results provided by Cusack et al. (2012) suggested that meteorology (in this case a

304   large increase in 2012; cf. Figure 2), changing from year to year, also determined the degree of comparability of

305   trends observed over different periods.

306   As reported in Fig. 2b, the $PM_{2.5}$ trends were linear for the three considered periods (1.2% < NL < 1.5%; cf. Table

307   1) and ME fits did not differ very much from MK fits (Fig. 2a). Following the MK and ME fits, the trends were

308   similar for the periods 2004 – 2014 and 2002 – 2014, whereas results were different for the period 2002 – 2010

309   (Cusack et al., 2012). MK test provided magnitudes of the trends of -1.87 %/yr (p<0.1) and -2.26 %/yr (p<0.05)

310   for 2004 – 2014 and 2002 – 2014, respectively. Conversely, the magnitude of the trend for the period 2002 –

311   2010 was higher in absolute values (-3.42 %/yr with p<0.01). Consequently, following the ME test, the

312   characteristic times (τ) of the periods 2004 – 2014 (31.7 yr) and 2002 – 2014 (34.2 yr) were similar and both

313   were higher compared with τ_1 calculated for the period 2002 – 2010 (19.3 yr). Consequently, the higher TR was

314   observed for the period 2002 – 2010 (34%) for which the highest slope was also observed following both MK

315   and ME tests. The RC was the lowest (9%) for the period 2002 – 2010 compared with 2004 – 2014 and 2002 –

316   2014 (15-16%). The differences observed in the magnitude of the trends and residual components for the three

317   periods are mostly due to the increase in the $PM_{2.5}$ concentrations observed in 2011-2012 when mean $PM_{2.5}$

318   reached around 15 $\mu g/m^3$ similar to the concentrations measured during 2002 – 2004 (around 14-16 $\mu g/m^3$).

319   Thus, over relatively short periods (9 -11 yr), the effects of just one meteorologically different year were clearly

320   visible. Despite this, we highlight that a statistically significant trend was observed thus confirming the

321   effectiveness of mitigation measures together with the effect of the economic crisis in Spain from 2008.

322

323   **3.3 Trends of chemical species**

324   The trends of the concentrations (using annual averages) of chemical species at BCN and MSY are reported in

325   Table 2 (for PM_{10}) and Table 3 (for $PM_{2.5}$). Figure 3 (for BCN) and Figure 4 (for MSY) show the trends of chemical

326   species in PM_{10}.

327   Here we assume that the change of the station in BCN in 2009 affected the trends of the concentrations of Cr,

328   Cu, Sn and Sb (traffic tracers), Al_2O_3, Ca, Mg, Ti, Rb, Sr (crustal elements related with both natural and

329   anthropogenic sources) and Fe (traffic and crustal tracer). These chemical species were highlighted in yellow in

330   Tables 2 and 3.

331   Figure 3 shows the impact of the change of the station for some of the aforementioned species in the year

332   2009. However, this change did not affect other species reported in Tables 2 and 3 and in Fig. 3, which had less

333   local character. These are SO_4^{2-}, NH_4^+, V, Ni (related with heavy oil combustion in the study area according to

10

Atmospheric
Chemistry
and Physics
Discussions

334 source apportionment results, cf. Par. 4), Pb, Cd, As and Zn (related with industrial/metallurgy activities), Na and

335 Cl (sea spray), and NO_3^-. Although nitrate particles in Barcelona were mainly from traffic, the concentrations of

336 these particles were not strongly affected by the change of the station due to their secondary origin. For the

337 aforementioned reasons the comparison between BCN and MSY will be performed only using species (and PMF

338 sources) not affected by the change of the station in BCN. The MSY station will be considered as reference

339 station given that no location changes occurred at this monitoring site during the study period.

340 For the industrial tracers (Pb, Cd, As) the trends were similar in both PM fractions at both BCN and MSY.

341 Following the MK test, the decreasing trends in PM_{10} fraction were statistically significant and ranged between -

342 3.43 %/yr (Cd and As; $p<0.001$) to -3.74 %/yr (Pb; $p<0.001$) at BCN and from -3.11 %/yr (Pb; $p<0.01$) to − 3.74

343 %/yr (As; $p<0.001$) at MSY. In $PM_{2.5}$ the magnitude of the trends were similar and ranged between -3.58 %/yr

344 (Cd; $p<0.001$) and -4.05 %/yr (Pb; $p<0.001$) at BCN and between -3.27 %/yr (As; $p<0.01$) and -3.74 %/yr (Pb;

345 $p<0.001$) at MSY. Similar magnitude of the trends for these species in both PM fractions at both sites confirmed

346 the common origin of these elements and the impact at regional scale of industrial sources.

347 However, it can be noted that the trends were not linear and the NL parameters were always higher than 10%

348 for Cd, Pb and As with the exception of As at MSY in PM_{10} (cf. Tables 2 and 3). Thus, for these industrial tracers

349 single or double exponential fits were on average needed indicating that the trends were not gradual and

350 consistent over time and that the effectiveness of the control measures for these pollutants were stronger at

351 the beginning of the period under study (2004-2009 approximately) compared to the end of the period (Figs. 3

352 and 4). This is also evident by comparing the linear MK fit (dashed black line) with the ME fit (red lines) in Figs. 3

353 and 4. Note that at BCN a double exponential (DE) fit was needed to simulate the trends of Pb and Cd

354 concentrations in PM_{10} likely because of the proximity of BCN measuring station to industrial emissions

355 compared to MSY station. For these industrial species in PM_{10} one of the two characteristic times (τ) was slightly

356 negative (cf. Tables 2) indicating both a slight increase of the simulated Pb and Cd concentrations in 2013-2014

357 and the strong decrease at the beginning of the period under study. Interestingly, as shown later, the PM_{10}

358 *Industrial/metallurgy* source contribution at BCN also showed a DE decreasing trend. The decrease observed for

359 Pb, Cd and As may be attributed to a decrease in the emissions from industrial production (smelters, Querol et

360 al., 2007) at a regional scale around Barcelona. The implementation of the IPPC Directive in 2008 in Spain is the

361 most probable cause for this downward trend. In PM_{10} the TR from ME test ranged between 67% for As and

362 73% for Pb, at BCN, and from 48% for As and 72% for Cd, at MSY. In $PM_{2.5}$ TRs were similar to those observed in

363 PM_{10} as expected given the general fine size mode of these industrial tracers (Table 1 and 2). The RC were quite

364 low and never exceeded 18% thus suggesting the goodness of the exponential fits used to study the trends of

365 the measured specie concentrations.

366 The comparison among the different ME trends in terms of characteristic times (τ) is complicated by the fact

367 that τ is especially sensitive to the noise introduced by the inter-annual variability over the period considered

368 here (11 years). However, some interesting features can be observed. Characteristic times in $PM_{2.5}$ were very

Atmospheric
Chemistry
and Physics
Discussions

369   similar for Pb and Cd at both stations (between 6.08 yr and 6.81 yr; cf. Table 3). For As in $PM_{2.5}$ the characteristic

370   times were similar between BCN (9.00 yr) and MSY (8.56 yr) but both were higher compared to Cd and Pb, due

371   to the slightly less intense exponential downward trend observed for As compared to Cd and Pb. Note that the

372   PMF analysis (cf. Paragraph 4) revealed that the concentrations of As were explained by multiple sources

373   (especially at BCN) whereas the *Industrial/metallurgy* source alone explained more than around 70% of Pb and

374   Cd concentrations (not shown). In PM_{10} in Barcelona the characteristic decreasing times for Pb, Cd and As were

375   similar to those calculated at the same station in $PM_{2.5}$ (despite the different exponential fits used), whereas at

376   MSY the PM_{10} characteristic times were slightly higher compared with $PM_{2.5}$ especially for As. It should be

377   considered that experimental uncertainties might also contribute to the observed differences in the

378   characteristic decreasing times over the period considered. Moreover, different sampling days for PM_{10} and

379    $PM_{2.5}$ together with possible sources of coarse As might also contribute to the observed differences.

380   In BCN the magnitude of the trend of PM_{10} Zn was -3.74 % (p<0.001), from the MK test, and it was comparable

381   with the magnitudes estimated for As, Cd and Pb. However, following the ME test, the trend was linear (NL=6%)

382   and the total reduction was lower (TR=50%) compared to the other industrial tracers. In $PM_{2.5}$ the magnitude of

383   the trend of Zn was lower (-2.65 %/yr; p<0.01) compared with As, Cd and Pb and, again, the trend was linear

384   (NL=5%) and the total reduction (TR=46%) was low compared to the other industrial tracers. At MSY, Zn in PM_{10}

385   showed no statistically decreasing linear trend (-1.40 %/yr; NL = 1%) with low TR of around 23%. Thus PM_{10} Zn

386   behaved clearly differently compared with As, Pb and Cd. The same was observed in $PM_{2.5}$ at MSY where the

387   magnitude of the trend for Zn (-2.02 %/yr; p<0.1 from MK test) was lower compared with As, Cd and Pb and

388   double exponential fit was needed following the ME test. As reported in Table 2, the two characteristics times

389   of the trend of Zn in $PM_{2.5}$ at MSY were positive and very much different. The exponent with lowest τ (0.21) was

390   needed to explain the strong decrease observed for $PM_{2.5}$ Zn between 2004 and 2005 (Figure SI-2). This

391   different behavior of Zn was likely due to the fact that Zn had multiple origins at both sites being related with

392   both industrial/metallurgy and road traffic emissions.

393   The concentrations of V and Ni in Barcelona in PM_{10} showed similar trends decreasing at a rate of -3.11 %/yr

394   (p<0.001) and -3.43 %/yr (p<0.001), respectively, following the MK test. Both elements had single-exponential

395   decreasing trends (NL = 12% and 11% for V and Ni, respectively) with very similar decreasing times (10.04 yr and

396   10.61 yr, respectively), TR (63% and 61%, respectively) and RC (17% and 16%, respectively), thus conforming the

397   common origin of these two elements. In $PM_{2.5}$ in Barcelona, the magnitude of the decreasing trends, following

398   the MK test, were slightly lower compared with PM_{10} (-2.96 %/yr and -3.11 %/yr for V and Ni, respectively;

399   p<0.01) and the trends were linear (NL = 9% for both elements). Characteristic times, TR and RC in $PM_{2.5}$ for V

400   and Ni in BCN were similar to those calculated in PM_{10}. Again we recall that the comparison of the fitting

401   parameters in PM_{10} and $PM_{2.5}$ might be affected by different number of samples available for these PM size

402   fractions. At MSY, V and Ni showed similar trends as in BCN in both PM fractions. The concentrations of V

403   decreased at the rate of -3.27 %/yr (p<0.01; linear trend with NL = 7%) and -2.65 %/yr (SE trend with NL = 10%)

404   in PM_{10} and $PM_{2.5}$, respectively. The concentrations of Ni decreased at the rate of -3.11 %/yr (p<0.01; linear

Atmospheric
Chemistry
and Physics
Discussions

405   trend with NL = 5%) and -2.80 %/yr (SE trend with NL = 13%) in PM_{10} and $PM_{2.5}$, respectively. Moreover, the

406   characteristic times τ, TR and RC for V and Ni calculated at MSY were similar to those calculated at BCN.

407   As stated before the trends for Cr, Sn, Cu and Sb, typical traffic tracers, were studied only for MSY station as a

408   consequence of the change of the station in BCN in 2009. Sn and Cu in PM_{10} at MSY showed very similar

409   behavior, both decreasing at the rate of -2.34 %/yr (p<0.05) with linear trends (2% < NL < 4%) and quite similar

410   TR (31-45%) and RC (15-19%). In $PM_{2.5}$, the concentrations of Sn and Cu at MSY showed marked trends

411   compared with PM_{10}, decreasing at -3.74 %/yr (p<0.001) and   -3.27 %/yr (p<0.01), respectively. In $PM_{2.5}$ the

412   trends were DE for Sn (see. Figure SI-3) and SE for Cu and TR (67-76%) and RC (9-13%) were similar for both

413   elements. The DE trend for $PM_{2.5}$ Sn at MSY was characterized (as for Zn) by a strong decrease between 2004

414   and 2005 and positive characteristic times (0.23 yr and 11.79 yr; cf. Figure SI-3). For Cr the situation was

415   different compared to Sn and Cu and in PM_{10} at MSY Cr showed no trend (0.00 %/yr). In $PM_{2.5}$ a slight and not

416   statistically significant decreasing trend was detected for Cr concentrations(-1.18 %/yr; p>0.1) which was linear

417   following the ME fit. In $PM_{2.5}$ the TR (31%) calculated for Cr was lower compared to Sn and Cu.

418   Sulfate (SO_4^{2-}) and ammonium (NH_4^+) particles concentrations showed very similar behavior in both $PM_{2.5}$ and

419   PM_{10} size fractions, due to their fine nature, at both sites. In BCN the magnitude of the trends were -3.74 %/yr

420   (p<0.001) and -3.58 %/yr (p<0.001) for SO_4^{2-} and NH_4^+, respectively. Both trends were SE with very similar

421   characteristic times (9.64-9.81 yr), NL (12%), TR (64-65%) and RC (12-14%). Very similar values were obtained

422   for these two species in $PM_{2.5}$ at BCN (cf. Table 3). At MSY both the magnitude of the trends of SO_4^{2-} and NH_4^+

423   from MK test and their statistically significance were lower compared to BCN in both fractions. The trends were

424   linear for SO_4^{2-} in both fractions and it was SE for NH_4^+. These differences could be explained by the distance of

425   MSY to direct specific sources of sulfate, such as shipping, compared to BCN, thus slightly reducing the

426   magnitude and the statistically significance of the trend of SO_4^{2-} at regional level. Similar result was observed for

427   the contribution of the *Ammonium sulfate* source at both sites (cf. Table 5) with slightly higher magnitude of the

428   trend observed at BCN compared to MSY. Possible reasons for the observed reduction in the concentrations of

429   ambient sulfate in and around Barcelona will be discussed later.

430   Fine NO_3^- (Table 3) showed very similar trends at both sites (-3.43 and -3.58 %/yr at MSY and BCN, respectively,

431   from MK test) with high statistical significance (p<0.001). At both stations NO_3^- trends were SE and showed

432   similar τ (5.81 yr and 7.61 yr), TR (82% and 73%) and RC (21% and 16%). In PM_{10} the trends of NO_3^- at BCN and

433   MSY were similar to those observed in $PM_{2.5}$ (-3.11 %/yr with p<0.01 from MK test). Following the ME test the

434   TR for PM_{10} NO_3^- were lower (54% at MSY and 64% at BCN) compared to $PM_{2.5}$ and the characteristic times in

435   PM_{10} were also lower compared to $PM_{2.5}$ at both sites. Thus, we deduced from ME analysis that fine NO_3^- had a

436   more pronounced downward trend compared to PM_{10} NO_3^- and mainly at MSY where τ $PM_{2.5}$ and τ PM_{10} were

437   5.81 yr and 12.71 yr, respectively. As reported in *Paragraph 4.1* statistically significant decreasing trends were

438   observed also for the *Ammonium Nitrate* source contributions at both sites. Possible reasons for the observed

Atmospheric
Chemistry
and Physics
Discussions

439   decreases of NO_3^- concentrations and *Ammonium Nitrate* source contributions will be discussed in *Paragraph.*

440   *4.1*.

441   As for Cr, Sn, Sb and Cu, the trends of mineral species (Al_2O_3, Ca, Fe) were studied only at MSY station. For these

442   elements, linear (with the exception of Al_2O_3 in $PM_{2.5}$ which was SE) and statistically significant decreasing

443   trends (with the exception of Ca in $PM_{2.5}$ with p>0.1) were detected. On average the TR were higher in the fine

444   fraction, ranging from 50% for Ca to 66% for Al_2O_3, compared to PM_{10} (16-38% cf. Table 2) thus likely suggesting

445   a decrease with time of the concentrations of anthropogenic mineral species from specific sources such as

446   cement and concrete production and production works. In fact, coarse mineral matter at regional background

447   sites is mainly of natural origin. Downward decreasing trend for mineral matter contribution in $PM_{2.5}$ at MSY

448   was also reported by Cusack et al. (2012) for the period 2002 – 2010 at the same station. It is probable that

449   variations in meteorological conditions from one year to another (i.e. intensity and frequency of Saharan dust

450   outbreaks) might also explain the observed trend of mineral tracers at regional level.

451   The concentrations of Cl^- did not show statistically significant trends in both fractions and at both sites due to its

452   main natural origin. Conversely, following the MK test, slightly statistical significant decreasing trends were

453   observed for Na at both sites and in both fractions with the exception of Na in PM_{10} at MSY for which no trend

454   was detected.

455   Finally, at MSY neither OC nor EC concentrations showed statistically significant trends (not shown). Consider

456   that the concentrations of EC at MSY are very low and around at 0.2-0.3 $\mu g/m^3$ as annual mean. Both

457   anthropogenic activity and biomass burning were expected to contribute to this chemical specie. Concerning OC

458   the lack of trend was probably due to the contribution from biogenic sources (and meteorology) to the

459   concentration of this specie at regional level.

460

461   **4. PMF source profiles and contributions**

462   Eight and seven sources were detected at BCN and MSY, respectively, in PM_{10} from PMF model. The absolute

463   and relative contributions of these sources to the measured PM_{10} mass are reported in Figure 5 and Table 4.

464   The chemical profiles of the detected sources were reported in Supporting Information (Figure SI-4).

465   Some of these sources were common at both BCN and MSY. These are: *Ammonium Sulfate* (secondary inorganic

466   source traced by SO_4^{2-} and NH_4^+ and contributing 3.95 $\mu g/m^3$ (23.7%) and 4.67 $\mu g/m^3$ (13.7%) at MSY and BCN,

467   respectively), *Ammonium nitrate* (secondary inorganic source traced by NO_3^- and NH_4^+ and contributing 1.31

468    $\mu g/m^3$ (7.9%) and 4.45 $\mu g/m^3$ (13.1%) at MSY and BCN, respectively), *V-Ni bearing* source (traced mainly by V, Ni

469   and SO_4^{2-} it represents the direct emissions from heavy oil combustion and contributed 0.71 $\mu g/m^3$ (4.3%) and

470   3.32 $\mu g/m^3$ (9.8%) at MSY and BCN, respectively), *Mineral* (traced by typical crustal elements such as Al, Ca, Ti,

471   Rb, Sr and contributing 2.70 $\mu g/m^3$ (16.2%) and 4.61 $\mu g/m^3$ (13.6%) at MSY and BCN, respectively), *Aged marine*

Atmospheric
Chemistry
and Physics
Discussions

Open Access
EGU

472　(traced by Na and Cl mainly with contributions from SO_4^{2-} and NO_3^- and contributing 1.76 $\mu g/m^3$ (10.6%) and

473　5.73 $\mu g/m^3$ (16.9%) at MSY and BCN, respectively). Sources detected at MSY but not at BCN were:

474　*Industrial/Traffic* source (traced by EC, OC, Cr, Cu, Zn, As, Cd, Sn, Sb and Pb it includes mixed contributions from

475　anthropogenic sources such as road traffic and metallurgic industries and contributed 1.43 $\mu g/m^3$ (8.6%)) and

476　*Aged organics* (traced mainly by OC and EC with maxima in summer indicating mainly a biogenic origin and

477　contributing 3.78 $\mu g/m^3$ (22.7%)). The ratio OC:EC in the *Industrial/Traffic* and *Aged organic* source profiles at

478　MSY were 4.2 and 11.7, respectively, thus indicating a strong influence of aged particles in the latter source with

479　the former source being more fresh. The statistic of the OC:EC ratio based on chemical data at MSY is reported

480　in Supporting Information (Figure SI-5). Mean and median values of OC:EC ratio at MSY were 9.1 and 7.8,

481　respectively.

482　Finally, some sources were detected at BCN but not at MSY: *traffic* (traced by C_{nm}, Cr, Cu, Sb and Fe mainly and

483　contributing 5.14 $\mu g/m^3$ (15.1%)), *road/work resuspension* (traced by both crustal elements, mainly Ca, and

484　traffic tracers such as Sb, Cu and Sn and contributing 4.25 $\mu g/m^3$ (12.5%)) and *Industrial/metallurgy* (traced by

485　Pb, Cd, As and Zn and contributing 0.96 $\mu g/m^3$ (2.8%).

486　A sensitivity study was performed in order to better interpret the PMF sources at BCN. In fact, for the period

487　2007 – 2014 separate OC and EC concentration measurements were available and a PMF was performed. The

488　comparison between the PMF source contributions obtained using the period 2007-2014 (separate OC and EC

489　measurements) and the whole period (2004-2014; C_{nm} (non-mineral carbon) available) is reported in Supporting

490　Information (Figure SI-6). As reported in Figure SI-6 the differences in source contribution and R^2 ranged

491　between -3% (*Mineral* source) and +20% (*Industrial* source) and 0.894 to 0.997, respectively, thus confirming

492　the correct interpretation of the 2004-2014 PMF sources where C_{nm} was used. The OC:EC ratio in the *Traffic*

493　source from 2007-2014 PMF was 1.70 (cf. Figure SI-7) whereas the mean and median OC:EC ratio from

494　chemistry data were 2.5 and 2.3, respectively, thus being in agreement with the contribution of fresh particles

495　from *Traffic* source at BCN.

496

4.1 Trends of PM_{10} source contributions: annual averages

498　Figures 6 and 7 and Table 5 show the results from MK and ME test applied to the annual averages of PM_{10}

499　source contributions at BCN and MSY. Following the MK test the source contributions that showed statistically

500　significant downward trends at both stations were *Ammonium sulfate*, *Ammonium nitrate*, and *V-Ni bearing*

501　sources. Moreover, statistically significant decreasing trends were observed for the *Industrial/Traffic* source

502　(including traffic and industrial emissions at MSY) and the *Industrial/metallurgy* source (at BCN). These sources

503　were clearly linked with anthropogenic activities and the observed decreasing trends confirmed the

504　effectiveness of pollution control measures discussed before and the possible effect of the economic crisis. The

505　contributions of these four sources at BCN were not affected by the change of the station in 2009 and,

Atmospheric
Chemistry
and Physics
Discussions

506 consequently, are discussed here. However, as already noted we cannot study trends for *Traffic*, *Road/work*

507 *resuspension* and *Mineral* source contributions at BCN.

508 Consistently with the trends of SO_4^{2-}, NO_3^- and NH_4^+ (Table 2), *Ammonium sulfate* and *Ammonium nitrate* source

509 contributions in PM_{10} showed highly statistically significant decreasing trends at both stations (Table 5). The

510 trends from MK test were -2.49 %/yr ($p<0.05$) and -3.74 %/yr ($p<0.001$) for *Ammonium sulfate* and *Ammonium*

511 *nitrates* contributions, respectively, at BCN and -2.02 %/yr ($p<0.05$) and -3.27 %/yr ($p<0.01$), respectively, at

512 MSY. At both stations the trend of the contribution of the *Ammonium sulfate* source to PM_{10} was DE (Double

513 Exponential) with two positive characteristic times (τ; Table 5) one of which was lower than the other

514 (especially at BCN) indicating a stronger decrease at the beginning of the considered period (cf. Figures 6 and 7).

515 Thus, the decrease over time of the contribution from the *Ammonium sulfate* source was not gradual and

516 monotonic. Note that at MSY there was a small statistically significant difference between SE and DE fits.

517 However, the DE fit was chosen reducing considerably the RC for this source. The TR was quite similar at both

518 sites: 67% at BCN and 51% at MSY and the RC was low at both sites (16-21%) again demonstrating the goodness

519 of the used fits. The observed decrease in the *Ammonium sulfate* source contribution may be attributed to the

520 legislation that came into force in 2007-2008 in Spain, the EC Directive on Large Combustion Plants, which

521 resulted in the application of flue gas desulfurization (FGD) systems in a number of large facilities in 2007-2008

522 in Spain. Moreover, from 2008 on, the use of heavy oils and petroleum coke for power generation was

523 forbidden around Barcelona, thus only natural gas was allowed to this end according to the 2008 Regional AQ

524 Plan.

525 *Ammonium nitrate* contribution trends were SE (Single Exponential) at both stations with very similar τ (8.96 yr

526 – 8.59 yr), TR (67-69 %) and RC (13-17%). Moreover, it should be noted that the lower MK magnitude (and

527 statistical significance) of the *Ammonium sulfate* contribution trends compared to the trends of the *Ammonium*

528 *nitrate* contributions was confirmed by the different fitting lines needed to fit these trends: double exponential

529 for *Ammonium sulfate* contributions and single exponential for *Ammonium* nitrate contributions. Thus, the

530 contributions to PM_{10} from the *Ammonium nitrate* source showed a more gradual and consistent over time

531 decrease compared to the contributions from the *Ammonium sulfate* source.

532 The decreases observed for the concentrations of nitrates (NO_3^-; cf. Par. 3.2) and for the contribution from the

533 *Ammonium Nitrate* source were mainly related to the reduction in ambient NO_x concentrations. Figure 8 shows

534 the levels of NO_2 from 2005 to 2014 in South Europe from NASA NO_2 OMI level3 plotted using the Giovanni

535 online data system (Acker and Leptoukh, 2007). In Spain it can be observed a general decrease of the

536 concentrations of NO_2 at regional level due to lower energy consumption mainly related with the financial crisis.

537 The decrease of NO_3^- concentrations and *Ammonium nitrate* source contributions around Barcelona was

538 attributed to the decrease of NO_x emissions mainly from the five power generation plants around the city.

539 Moreover, during 2008-2012 the Regional AQ Plan has driven the implementation of SCRT (continuously

Atmospheric
Chemistry
and Physics
Discussions

540   regenerating PM traps with selective catalytic reduction for NO_2) and the hybridization and shift to natural gas

541   engines of the Barcelona´s bus fleet may have had also an influence in NO_x ambient concentrations.

542   The decreasing trends of the *V-Ni bearing* source from MK analysis were similar at both stations and around -

543   3.11 %/yr at BCN (p<0.01) and -2.96 %/yr (p<0.01) at MSY. The trends were linear (L) at MSY (NL=8%) and SE at

544   BCN (NL=11%). Very similar characteristic times (τ) were observed at both stations for the *V-Ni bearing* source

545   contributions: 10.59 yr at BCN and 11.94 yr at MSY. Interestingly, the τ calculated for the V-Ni bearing source

546   were very similar to those calculated for V and Ni species in PM_{10} (cf. Table 2). The *V-Ni bearing* TR was around

547   61% at BCN and 57% at MSY and RCs were similar (19-25 %). Note that following the MK test the magnitude of

548   the trends for these three sources were on average higher at BCN compared to MSY likely due to the proximity

549   of the BCN measuring station to anthropogenic sources of V and Ni (mainly shipping). The observed decrease in

550   the *V-Ni bearing* source contribution was mainly attributed to the ban of the use of heavy oils and petroleum

551   coke for power generation from 2008.

552   The *Industrial/Metallurgy* source contribution at BCN decreased at the rate of -3.43 %/yr from MK test

553   (p<0.001). As already observed this decrease was mainly attributed to the implementation of IPPC Directives.

554   Moreover, the observed decrease may be attributed to a decrease in the emissions from industrial production

555   (smelters, Querol et al., 2007) at a regional scale around Barcelona. The implementation of the IPPC Directive in

556   2008 in Spain was the most probable cause for this downward trend. Also for this source the trend was DE with

557   one negative characteristic time (cf. Table 5) due to a slight increase of the *Industrial/Metallurgy* source

558   contribution at the end of the considered period. This was consistent with the trends observed for the *Industrial*

559   tracers at BCN (cf. Figure 3 and Table 2). TR and RC for the *Industrial* source contributions at BCN were 56% and

560   11%, respectively. Note again that low RC indicates a good fit of the data using the multi-exponential approach.

561   Interestingly, the contribution of the *Industrial/Traffic* source at MSY had a very similar magnitude of the trend

562   (-3.11 %/yr from MK test with p<0.01) compared to the BCN *Industrial* contribution trend, being both sources

563   traced mostly by the same industrial tracers. Also the TR and RC were similar (54% and 11%, respectively at

564   MSY).

565   At MSY the contribution of the *Aged organics* source increased at the rate of +1.25 %/yr however the trend was

566   not statistically significant. The increasing trend for this source was mainly due to the observed increase in the

567   contribution in the year 2011 when mean annual OC concentration at MSY reached a maximum in the

568   considered 11-yr period (not shown). The *Aged organic* source contribution (likely mainly driven by biogenic

569   POA and SOA formed in these forested regional area in the WMB, cf. Pandolfi et al., 2014) did not show

570   statistically significant trends being these contributions mainly driven by meteorology.

571   The *Mineral* source contribution at MSY showed statistically significant decreasing trend (p<0.1) whereas the

572   *Marine* source contributions showed no-statistically significant trends at both stations this being consistent with

573   the natural origin of this latter source. The statistically significant decreasing trend observed at MSY for the

574   *Mineral* source was in agreement with what observed at the same station by Cusack et al. (2012). This

Atmospheric
Chemistry
and Physics
Discussions

575   decreasing trend could be due to a possible decrease of the emissions of anthropogenic mineral species from

576   specific sources such as cement and concrete production and construction works.

577   Finally, the possible relationship of the ambient air pollution trends with the emission patterns by sectors is

578   evaluated here using the NECo statistical data for Spain (MINETUR, 2013) as well as of the time trends for SO_2

579   and NO_x emissions evidenced for the NEIs (MAGRAMA, 2013). The primary energy consumption increased by

580   +4% from 2004 to 2007, slightly decreased from 2007 to 2008 (−4%), and markedly decreased in 2009 (−12%

581   with respect to 2007) (Fig. 9). Since 2009, the energy consumption indicator seems to remain constantly low

582   until 2012 with an additional decrease in 2013 and 2014 (around -8% compared to 2009). Oil consumption was

583   fairly constant during 2004–2007 showing an important (−29%) decrease during 2007–2014, without major

584   changes from 2007 to 2008 (−3%). This trend is probably governed by the fuel consumption for traffic road.

585   Natural gas consumption increased (+39%) from 2004 to 2008, and then diminished by -45% in 2014 compared

586   to 2008. Coal consumption remained constantly high from 2004 to 2007 whereas, as for the emissions of SO_2

587   (Fig. 10), a sharp decrease occurred from 2007 to 2008 (−31%), continuing until 2010 (−61% compared to 2007).

588   However, in the period 2011-2014 there was an important increase leading to an average consumption similar

589   to the consumption for the year 2008. Nuclear energy consumption remained relatively constant along the

590   study period, whereas the hydroelectric generation had three maxima in 2010, 2013 and 2014, coinciding with

591   the fall of coal consumption. The 2010 increase of hydroelectric consumption was very remarkable and due to

592   the high rainfall rate of this year. Thus, 2010 was a favorable year for atmospheric dispersion and washout of

593   pollution in Spain, but air quality also improved by lower atmospheric emissions due to the decrease of coal

594   consumption in favor of a hydroelectric growth. Renewable energy consumption increased by 440% from 2004

595   to 2014, with a gradual growth in the NECo.

596

597   **5.0 Conclusions**

598   PM chemical speciated data collected at two twin stations in NE of Spain (one urban background station and

599   one regional background station) during 2004 – 2014 were used to study trends of source contributions from

600   PMF analysis and of chemical species concentrations. Despite the fact the trends of different PM fractions (PM_1,

601    $PM_{2.5}$ and PM_{10}) were linear during the period under study, the trends of specific chemical elements and source

602   contributions were single or double exponential demonstrating the different effectiveness and time of

603   implementation of different reduction strategies on specific pollutant sources. The contributions that showed

604   statistically significant downward trends at both Barcelona (BCN; UB) and Montseny (MSY; RB) were from

605   *Ammonium sulfate*, *Ammonium nitrate*, and *V-Ni bearing* sources. Moreover, statistically significant decreasing

606   trends were observed for the *Industrial/Traffic* source (at MSY; mixed road traffic and metallurgy) and the

607   *Industrial/metallurgy* source (at BCN). These sources were clearly linked with anthropogenic activities and the

608   observed decreasing trends confirmed the effectiveness of pollution control measures implemented at EU or

609   regional/local levels. Moreover, the economic crisis which started in 2008 in Spain also contributed to the

Atmospheric
Chemistry
and Physics
Discussions

Open Access

EGU

610 observed trends. The general trends observed for the calculated PMF source contributions well reflected the

611 trends observed for the chemical tracers of these pollutant sources. At both sites the decreasing trends of the

612 *Ammonium sulfate* source contributions were double exponential indicating that the trends were not gradual

613 and consistent with time. In fact, the observed decrease in the *Ammonium sulfate* source contribution was

614 mainly attributed to the EC Directive on Large Combustion Plants implemented from 2008 in Spain, resulting in

615 the application of fuels gas desulfurization (FGD) systems in a number of large facilities. Moreover, the use of

616 heavy oils and petroleum coke for power generation was forbidden around Barcelona from 2008, thus only

617 natural gas was allowed to this end according to the 2008 Regional AQ Plan. Conversely, *Ammonium nitrate* and

618 *V-Ni bearing* source contributions were well fitted by a single exponential curve suggesting a more gradual and

619 consistent with time decreasing trends for these contributions compared to *Ammonium sulfate* source

620 contribution. The decrease observed for the contribution of the *Ammonium Nitrate* source was mainly due to

621 the reduction in ambient NO_x concentrations. In Spain a general decrease of the concentrations of NO_2 at

622 regional level was observed and it was mainly related with the lower energy consumption related with the

623 financial crisis. The decrease of nitrates concentrations and *Ammonium nitrate* source contributions around

624 Barcelona was also attributed to the decrease of NO_x emissions from the five power generation plants around

625 the city. Moreover, a Regional AQ Plan implementing the SCRT (continuously regenerating PM traps with

626 selective catalytic reduction for NO_2) and the hybridization and shift to natural gas engines of the Barcelona´s

627 bus fleet may have had also an influence in NO_x ambient concentrations. The magnitude of the decreasing

628 trends of the contributions of the aforementioned sources were always higher at BCN compared to MSY likely

629 because of the proximity of the BCN measurement site to anthropogenic pollutant sources compared to the

630 MSY site.

631

632 **Acknowledgments.**

642

643

Atmospheric
Chemistry
and Physics
Discussions

Open Access

EGU

644 **Bibliography**

645 Acker J. G. and G. Leptoukh, *Online Analysis Enhances Use of NASA Earth Science Data*, Eos, Trans. AGU, 88, 2,

646 14-17, 2007.

647 Alastuey, A., Minguillón, M.C., Pérez, N., Querol, X., Viana, M. and de Leeuw, F. (2011). *PM10 Measurement*

648 *Methods and Correction Factors: 2009 Status Report*, ETC/ACM Technical Paper 2011/21, 2011.

649 Amato, F., M. Pandolfi, A. Escrig, X. Querol, A. Alastuey, J. Pey, N. Perez, P.K. Hopke, *Quantifying road dust*

650 *resuspension in urban environment by Multilinear Engine: A comparison with PMF2*, Atmospheric Environment.

651 43 - 17, pp. 2770 - 2780. 06/2009, 2009.

652 Barmpadimos, I., J. Keller, D. Oderbolz, C. Hueglin, A.S.H. Prevot, *One decade of parallel fine ($PM_{2.5}$) and coarse*

653 *(PM_{10}–$PM_{2.5}$) particulate matter measurements in Europe: trends and variability*, Atmos Chem Phys, 12 (2012),

654 pp. 3189–3203 http://dx.doi.org/10.5194/acp-12-3189-2012.

655 Carslaw, D.C., *The OpenAir manual — open-source tools for analysing air pollution data*, Manual for version 0.5-

656 16, King's College, London (2012).

657 Carslaw, D.C., K. Ropkins, *OpenAir — an R package for air quality data analysis,* Environ Model Softw, 27–28

658 (2012), pp. 52–61.

659 Cusack, M., A. Alastuey, N. Perez, J. Pey, X. Querol, *Trends of particulate matter (PM2.5) and chemical*

660 *composition at a regional background site in the Western Mediterranean over the last nine years (2002–2010)*,

661 Atmos Chem Phys, 12 (2012), pp. 8341–8357 http://dx.doi.org/10.5194/acp-12-8341-2012 [www.atmos-chem-

662 phys.net/12/8341/2012/]

663 EEA: European Environmental Agency Air quality in Europe — 2013 report, EEA report 9/2013, Copenhagen,

664 1725-9177 (2013) [107 pp. http://www.eea.europa.eu/publications/air-quality-in-europe-2013].

665 EEA: European Environmental Agency Air quality in Europe — 2015 report, *Many Europeans still exposed to*

666 *harmful air pollution. Air pollution is the single largest environmental health risk in Europe*, EEA report 11/2015,

667 Copenhagen, 1-7 (2015) [http://www.eea.europa.eu/media/newsreleases/many-europeans-still-exposed-to-

668 air-pollution-2015].

669 Escrig, A., Monfort, E., Celades, I., Querol, X., Amato, F., Min guillon, M. C., and Hopke, P. K.: Application of

670 optimally scaled target factor analysis for assessing source contribution of ambi ent PM10, J. Air Waste

671 Manage., 59(11), 1296–1307, 2009.

672 Gilbert, R.O. 1987 . Statistical Methods for Environmental Pollution Monitoring, Wiley, NY.

Atmospheric
Chemistry
and Physics
Discussions

673   Guerreiro, C., Leeuw, F. de, Foltescu, V., Horálek, J., & European Environment Agency. (2014). *Air quality in*

674   *Europe   2014   report*,   Luxembourg: Publications   Office.   Retrieved   from

675   http://bookshop.europa.eu/uri?target=EUB:NOTICE:THAL14005:EN:HTML.

676   Harrison, R.M., J. Stedman, D. Derwent, *New directions: why are PM10 concentrations in Europe not falling?*,

677   Atmos Environ, 42 (3) (2008), pp. 603–606.

678   Henschel, S., X. Querol, R. Atkinson, M. Pandolfi, A. Zeca, A. Le Tertre, A. Analitis, K. Katsouyanni, O. Chanel, M.

679   Pascal, C. Bouland, D. Haluza, S. Medina, P.G. Goodman, *Ambient air SO2 patterns in 6 European cities*,

680   Atmospheric Environment. 79, pp. 236 - 247. 11/2013, 2013.

681   Henschel, S., A. Le Tertre, R.W. Atkinson, X. Querol, M. Pandolfi, A. Zeka, D. Haluza, A. Antonis, K. Katsouyanni,

682   C. Bouland, M. Pascal, S. Medina, P.G. Goodman, *Trends of nitrogen oxides in ambient air in nine European cities*

683   *between 1999 and 2010*, Atmospheric Environment. 117, pp. 234 - 241. 09/2015, 2015.

684   Kendall, M.G. 1975. Rank Correlation Methods, 4th edition, Charles Griffin, London.

685   Mann, H.B. 1945. Non-parametric tests against trend, Econometrica 13:163-171.

686   Paatero, P. and Tapper, U.: *Positive Matrix Factorization: a non negative factor model with optimal utilization of*

687   *error estimates of data values*, Environmetrics, 5, 111–126, 1994.

688   Paatero, P.: *Least squares formulation of robust non-negative factor analysis*, Chemometr. Intell. Lab., 37, 23–

689   35, 1997.

690   Paatero, P., Hopke, P. K., Song, X., and Ramadan, Z.: *Understanding and controlling rotations in factor analytic*

691   *models*, Chemo metrics and Intelligent Laboratory Systems, 60(1–2), 253–264, 2002.

692   Paatero, P. and Hopke, P. K.: *Discarding or downweighting high noise variables in factor analytic models*, Anal.

693   Chim. Acta, 490, 277–289, doi:10.1016/s0003-2670(02)01643-4, 2003.

694   Paatero, P., Hopke, P. K., Begum, B. A., and Biswas, S. K.: *A graphical diagnostic method for assessing the*

695   *rotation in factor analytical models of atmospheric pollution*, Atmos. Environ., 39, 193–201,

696   doi:10.1016/j.atmosenv.2004.08.018, 2005.

697   Pandolfi, M., Cusack, M., Alastuey, a. and Querol, X.: Variability of aerosol optical properties in the Western

698   Mediterranean Basin, Atmos. Chem. Phys., 11(15), 8189–8203, doi:10.5194/acp-11-8189-2011, 2011.

699   Pandolfi, M., F. Amato, C. Reche, A. Alastuey, R. P. Otjes, M. J. Blom, X. Querol, *Summer ammonia*

700   *measurements in a densely populated Mediterranean city*, Atmospheric Chemistry and Physics. 12, pp. 7557 -

701   7575. 08/2012, 2012.

702   Pandolfi, M., G. Martucci, X. Querol, A. Alastuey, F. Wilsenack, S. Frey, C.D. O'Dowd, M. Dall'Osto, *Continuous*

703   *atmospheric boundary layer observations in the coastal urban area of Barcelona during SAPUSS*, Atmospheric

704   Chemistry and Physics. 13 - 9, pp. 4983 - 4996. 05/2013, 2013.

705   Pandolfi, M., Querol, X., Alastuey, A., Jimenez, J. L., Jorba, O., Day, D., Ortega, A., Cubison, M. J., Comerón, A.,

706   Sicard, M., Mohr, C., Prévôt, A. S. H., Minguillón, M. C., Pey, J., Baldasano, J. M., Burkhart, J. F., Seco, R.,

707   Peñuelas, J., van Drooge, B. L., Artiñano, B., Di Marco, C., Nemitz, E., Schallhart, S., Metzger, A., Hansel, A.,

708   Lorente, J., Ng, S., Jayne, J. and Szidat, S.: Effects of sources and meteorology on particulate matter in the

709   Western Mediterranean Basin: An overview of the DAURE campaign, J. Geophys. Res. Atmos., 119(8), 4978–

710   5010, doi:10.1002/2013JD021079, 2014.

711   Pérez, N., Pey, J., Castillo, S., Viana, M., Alastuey, A. and Querol, X.: Interpretation of the variability of levels of

712   regional background aerosols in the Western Mediterranean, Sci. Total Environ., 407(1), 527–540,

713   doi:10.1016/j.scitotenv.2008.09.006, 2008.

714   Pey, J., Pérez, N., Querol, X., Alastuey, A., Cusack, M. and Reche, C.: Intense winter atmospheric pollution

715   episodes affecting the Western Mediterranean., Sci. Total Environ., 408(8), 1951–9,

716   doi:10.1016/j.scitotenv.2010.01.052, 2010.

717   Querol, X., A. Alastuey, T. Moreno, M.M. Viana, S. Castillo, J. Pey, et al., *Spatial and temporal variations*

718   *inairborne particulate matter (PM10 and PM2.5) across Spain 1999–2005*, Atmos Environ, 42 (2008), 3694–

719   3979.

720   Querol, X., M. Viana, T. Moreno, A. Alastuey, J. Pey, F. Amato, M. Pandolfi, et al., *Scientific bases for a National*

721   *Air Quality Plan* (in Spanish), Colección Informes CSIC, 978-84-00-09475-1, 3 (2012) [349 pp.].

722   Querol, X., , A. Alastuey, M. Pandolfi, C. Reche, N. Pérez, M.C. Minguillón, T. Moreno, M. Viana, M. Escudero, A.

723   Orio, M. Pallarés, F. Reina, *2001–2012 trends on air quality in Spain*, Science of The Total Environment, 490,

724   (2014), 957–969, doi:10.1016/j.scitotenv.2014.05.074.

725   Salvador P., Artíñano B., Viana M., Alastuey A., Querol X.: *Evaluation of the changes in the Madrid metropolitan*

726   *area influencing air quality: analysis of 1999-2008 temporal trend of Particulate Matter*, Atmos. Environ., 57,

727   175-185, 2012.

728

729   Sen, P.K., *Estimates of regression coefficient based on Kendall's tau*, J Am Stat Assoc, 63 (1968), pp. 1379–1389.

730   Shatalov V., Ilyin I., Gusev A., Rozovskaya O., Travnikov O.: *Heavy Metals and Persistent Organic Pollutants:*

731   *development of multi-scale modeling and trend analysis methodology.* EMEP/MSC-E Technical report 1/2015,

732   2015.

Atmospheric
Chemistry
and Physics
Discussions

733   Smith, D.M.: *Computing single parameter transformations*, Communications in Statistics - Simulation and

734   Computation, 32, 605-618, 2002.

735   Theil, H., *A rank invariant method of linear and polynomial regression analysis, I, II, III,* Proceedings of the

736   Koninklijke Nederlandse Akademie Wetenschappen, SeriesA — Mathematical Sciences, 386–392, 521–525,

737   1397–1412 (1950).

738   Williams, M.L., D. Carslaw, *New directions: science and policy — out of step on NOx and NO2?* Atmos Environ, 45

739   (23) (2011), pp. 3911–3912.

740

741

742

743

744

745

746

747

748

749

750

751

752

753

754

755

756

757

758

Atmospheric
Chemistry
and Physics
Discussions

Table 1: Mann-Kendall and Multi-exponential trends of different PM fractions from both gravimetry (grav) and optical (OPC) measurements at BCN (bold italic) and MSY (2004-2014). Type: linear (L), single-exponential (SE), double exponential (DE); a (μgm^{-3}) and τ (yr) are the constant and the characteristic time, respectively, of the exponential fit of the data; NL (%) = Non-Linearity; TR (%) = Total Reduction; RC (%) = Residual Component. Significance of the trends following the Mann-Kendall test: *** (p-value < 0.001), ** (p-value < 0.01), * (p-value < 0.05), + (p-value < 0.1).

PM_x Fraction	PM_x Conc. 2004 (μgm^{-3})	PM_x Conc. 2014 (μgm^{-3})	Mann-Kendall fit Trend (%/yr)	Mann-Kendall fit p-value	Multi-exponential fit type	Multi-exponential fit a (μgm^{-3})	Multi-exponential fit τ (yr)	NL (%)	TR (%)	RC (%)
PM$_{10}$ (grav)	*41.12*	*19.16*	*-3.58*	***	*L*	*50.30*	*11.60*	*9*	*58*	*10*
	19.24	13.88	-0.47		L	17.92	79.46	0	12	17
PM$_{2.5}$ (grav)	*31.61*	*13.18*	*-3.89*	***	*L*	*32.41*	*10.87*	*9*	*60*	*8*
	16.18	9.80	-1.87	+	L	14.36	31.70	1	27	16
PM$_{10}$ (OPC)	*39.06*	*19.84*	*-3.43*	***	*L*	*45.85*	*15.62*	*5*	*47*	*11*
	18.63	12.34	0.00		L	16.25	115.92	0	8	15
PM$_{2.5}$ (OPC)	*27.12*	*12.86*	*-3.11*	**	*L*	*29.33*	*15.51*	*5*	*53*	*11*
	15.71	9.28	-1.78	+	L	12.46	40.59	0	24	14
PM$_1$ (OPC)	*20.78*	*9.05*	*-3.11*	**	*L*	*23.03*	*13.83*	*6*	*51*	*13*
	12.86	6.68	-1.25		L	10.90	37.33	1	23	17
PM$_{1-10}$ (OPC)	*18.29*	*11.48*	*-2.34*	*	*L*	*22.86*	*17.92*	*4*	*43*	*16*
	5.94	5.51	0.93		L	5.61	-68.77	0	-16	23
PM$_{1/10}$ (OPC)	*0.55*	*0.46*	*-0.31*		*L*	*0.50*	*135.80*	*0*	*7*	*9*
	0.71	0.59	-1.25		L	0.67	70.88	0	13	10
PM$_{2.5-10}$ (OPC)	*13.07*	*7.89*	*-2.18*	*	*L*	*14.72*	*16.25*	*5*	*46*	*18*
	4.09	3.79	0.62		L	3.88	-76.32	0	-14	26
PM$_{2.5/10}$ (OPC)	*0.66*	*0.63*	*-0.62*		*L*	*0.68*	*396.60*	*0*	*2*	*4*
	0.80	0.77	-0.62		L	0.76	288.49	0	3	9

759
760
761
762
763

764

765

766

767

768

769

770

771

772

773

774

Atmospheric
Chemistry
and Physics

Discussions

Open Access

775 **Table 2**: Mann-Kendall and Multi-exponential trends of different chemical species in PM_{10} at BCN (bold italic) and MSY. Colour highlights
776 species in BCN for which trends cannot be studied due to the change of the BCN station in 2009. Type: linear (L), single-exponential (SE),
777 double exponential (DE); **a** (μgm^{-3}) and τ (yr) are the constants and the characteristic times, respectively, of the exponential data fittings;
778 NL (%) = Non-Linearity; TR (%) = Total Reduction; RC (%) = Residual Component. Significance of the trends following the Mann-Kendall
779 test: *** (p-value < 0.001), ** (p-value < 0.01), * (p-value < 0.05), + (p-value < 0.1).

| Specie | PM_{10} (*BCN*;MSY) | | Mann-Kendall fit | | Multi-exponential fit | | | | | |
	Concentration 2004 (μgm^{-3})	Concentration 2014 (μgm^{-3})	Trend (%/yr)	p-value	type	a (μgm^{-3})	τ (yr)	NL (%)	TR (%)	RC (%)
Pb	*0.02685*	*0.00694*	*-3.74*	***	*DE*	*0.03409* / *1.64E-5*	*5.38* / *-2.09*	*39*	*73*	*10*
Pb	0.00481	0.00190	-3.11	**	SE	0.00553	10.22	11	62	13
Cd	*0.00043*	*0.00015*	*-3.43*	***	*DE*	*0.00051* / *3.36E-8*	*6.64* / *-1.48*	*33*	*65*	*11*
Cd	0.00017	0.00006	-3.27	**	SE	0.00018	7.92	18	72	16
As	*0.00094*	*0.00036*	*-3.43*	***	*SE*	*0.00118*	*9.11*	*14*	*67*	*11*
As	0.00029	0.00017	-3.74	***	L	0.00031	15.39	5	48	10
Zn	*0.10584*	*0.05483*	*-3.74*	***	*L*	*0.11310*	*14.49*	*6*	*50*	*7*
Zn	0.01401	0.00912	-1.40		L	0.01434	38.46	1	23	19
V	*0.01116*	*0.00454*	*-3.11*	**	*SE*	*0.01502*	*10.04*	*12*	*63*	*17*
V	0.00328	0.00175	-3.27	**	L	0.00412	13.00	7	54	16
Ni	*0.00531*	*0.00284*	*-3.43*	***	*SE*	*0.00678*	*10.61*	*11*	*61*	*16*
Ni	0.00155	0.00100	-3.11	**	L	0.00180	15.73	5	47	21
Cr	*0.00499*	*0.00316*	*-2.49*	*	*L*	*0.00641*	*15.38*	*5*	*48*	*18*
Cr	0.00102	0.00110	0.00		L	0.00100	127.74	0	8	23
Sn	*0.00532*	*0.00402*	*-2.02*	*	*L*	*0.00745*	*24.55*	*2*	*33*	*15*
Sn	0.00127	0.00057	-2.34	*	L	0.00107	16.97	4	45	15
Cu	*0.07064*	*0.01394*	*-2.96*	**	*SE*	*0.10238*	*6.18*	*27*	*80*	*30*
Cu	0.00420	0.00216	-2.34	*	L	0.00416	26.63	2	31	19
Sb	*0.00894*	*0.00207*	*-2.96*	**	*SE*	*0.01140*	*6.19*	*27*	*80*	*25*
Sb	0.00058	0.00025	-2.80	**	SE	0.00064	10.46	11	62	13
SO_4^{2-}	*5.74436*	*2.28596*	*-3.74*	***	*SE*	*6.56033*	*9.81*	*12*	*64*	*12*
SO_4^{2-}	2.84849	1.67712	-2.80	**	L	3.00501	18.54	4	42	19
NO_3^-	*5.07816*	*1.72401*	*-3.11*	**	*SE*	*6.49890*	*9.83*	*12*	*64*	*15*
NO_3^-	1.80724	0.67419	-3.11	**	L	2.10077	12.71	7	54	14
NH_4^+	*1.92062*	*0.57008*	*-3.58*	***	*SE*	*1.90645*	*9.64*	*12*	*65*	*14*
NH_4^+	1.14268	0.40135	-2.49	*	SE	1.28868	9.26	13	66	22
Al_2O_3	*1.25631*	*0.42353*	*-2.34*	*	*SE*	*1.83628*	*8.80*	*15*	*68*	*33*
Al_2O_3	0.72357	0.46382	-2.18	*	L	0.71956	23.71	2	35	19
Ca	*2.34383*	*0.49357*	*-2.96*	**	*SE*	*3.35120*	*7.27*	*21*	*75*	*34*
Ca	0.42703	0.28279	-2.49	*	L	0.47048	21.07	3	38	17
Fe	*0.94101*	*0.46700*	*-2.18*	*	*L*	*1.21322*	*11.22*	*9*	*59*	*17*
Fe	0.22371	0.14895	-1.71	+	L	0.22198	56.84	0	16	40
Na	*1.02188*	*0.77408*	*-2.34*	*	*L*	*1.13649*	*28.31*	*2*	*30*	*13*
Na	0.31184	0.33089	0.00		L	0.33531	493.40	0	2	21
Cl	*0.85827*	*0.78893*	*-1.09*		*L*	*0.92544*	*40.26*	*1*	*22*	*20*
Cl	0.17991	0.34437	0.62		L	0.22167	-36.01	1	-32	61

780

781

782

783

784

785

786

Atmospheric
Chemistry
and Physics
Discussions

787 **Table 3**: Mann-Kendall and Multi-exponential trends of different chemical species in PM$_{2.5}$ at BCN (bold italic) and MSY. Colour highlights
788 species in BCN for which trends cannot be studied due to the change in the BCN station in 2009. Type: linear (L), single-exponential (SE),
789 double exponential (DE); **a** (μgm^{-3}) and τ (yr) are the constants and the characteristic times, respectively, of the exponential data fittings;
790 NL (%) = Non-Linearity; TR (%) = Total Reduction; RC (%) = Residual Component. Significance of the trends following the Mann-Kendall
791 test: *** (p-value < 0.001), ** (p-value < 0.01), * (p-value < 0.05), + (p-value < 0.1).

Specie	PM$_{2.5}$ (*BCN*;MSY) Concentration 2004 (μgm^{-3})	Concentration 2014 (μgm^{-3})	Mann-Kendall fit Trend (%/yr)	p-value	Multi-exponential fit type	a (μgm^{-3})	τ (yr)	NL (%)	TR (%)	RC (%)
Pb	*0.02117*	*0.00500*	*-4.05*	***	*SE*	*0.02390*	*6.24*	*27*	*80*	*13*
	0.00642	0.00149	-3.74	***	SE	0.00716	6.08	28	81	18
Cd	*0.00041*	*0.00011*	*-3.58*	***	*SE*	*0.00047*	*6.81*	*23*	*77*	*13*
	0.00020	0.00005	-3.58	***	SE	0.00020	6.77	23	77	18
As	*0.00069*	*0.00027*	*-3.74*	***	*SE*	*0.00091*	*9.00*	*14*	*67*	*11*
	0.00029	0.00013	-3.27	**	SE	0.00033	8.56	15	69	19
Zn	*0.07500*	*0.03985*	*-2.65*	**	*L*	*0.07330*	*16.41*	*5*	*46*	*13*
	0.02649	0.01017	-2.02	*	DE	1.53281 / 0.01377	0.21 / 22.56	49	68	18
V	*0.00823*	*0.00368*	*-2.96*	**	*L*	*0.01121*	*11.13*	*9*	*59*	*16*
	0.00271	0.00130	-2.65	**	SE	0.00338	10.77	10	60	21
Ni	*0.00402*	*0.00185*	*-3.11*	**	*L*	*0.00498*	*11.23*	*9*	*59*	*15*
	0.00189	0.00080	-2.80	**	SE	0.00205	9.36	13	42	24
Cr	*0.00226*	*0.00155*	*-1.40*		*L*	*0.00297*	*16.05*	*5*	*46*	*27*
	0.00077	0.00062	-1.18		L	0.00104	16.75	4	31	24
Sn	*0.00268*	*0.00188*	*-2.34*	*	*L*	*0.00398*	*19.87*	*3*	*40*	*16*
	0.00157	0.00043	-3.74	***	DE	0.04830 / 0.00100	0.23 / 11.79	44	76	9
Cu	*0.02747*	*0.00503*	*-3.11*	**	*SE*	*0.05273*	*5.32*	*34*	*85*	*43*
	0.00394	0.00113	-3.27	**	SE	0.00426	8.99	14	67	13
Sb	*0.00300*	*0.00078*	*-2.96*	**	*DE*	*0.00395* / *1.6E-6*	*5.10* / *-1.98*	*42*	*73*	*18*
	0.00053	0.00015	-2.80	**	DE	0.00069 / 1.3E-6	4.52 / -2.50	48	70	16
SO$_4$$^{2-}$	*4.86564*	*1.92388*	*-3.74*	***	*SE*	*5.64582*	*9.69*	*12*	*64*	*9*
	2.98922	1.43381	-2.96	**	L	3.29195	11.70	9	57	16
NO$_3$$^{-}$	*3.45513*	*0.86002*	*-3.58*	***	*SE*	*4.14459*	*7.61*	*19*	*73*	*16*
	1.66095	0.29452	-3.43	***	SE	1.96014	5.81	30	82	21
NH$_4$$^{+}$	*2.19735*	*0.68393*	*-3.58*	***	*SE*	*2.27813*	*10.53*	*11*	*61*	*15*
	1.39366	0.48049	-3.11	**	SE	1.62588	7.94	18	72	14
Al$_2$O$_3$	*0.46954*	*0.14567*	*-2.65*	**	*SE*	*0.73949*	*7.46*	*20*	*74*	*39*
	0.30245	0.10153	-2.34	*	SE	0.26678	9.36	13	66	35
Ca	*0.65421*	*0.13737*	*-2.80*	**	*SE*	*1.09283*	*5.91*	*29*	*82*	*46*
	0.11478	0.06540	-1.56		L	0.10688	14.36	6	50	33
Fe	*0.32489*	*0.15007*	*-1.87*	+	*SE*	*0.45302*	*8.26*	*16*	*70*	*25*
	0.09679	0.03716	-2.02	*	L	0.08842	12.20	8	56	31
Na	*0.27476*	*0.17863*	*-1.87*	+	*L*	*0.32279*	*19.56*	*3*	*40*	*15*
	0.13091	0.07252	-2.49	*	L	0.13516	18.56	4	42	19
Cl	*0.37296*	*0.32756*	*-0.47*		*L*	*0.37806*	*23.25*	*2*	*35*	*49*
	0.10917	0.18225	0.00		L	0.16170	-1029.00	0	-1	79

792

793

794

795

796

Atmospheric
Chemistry
and Physics
Discussions

797   **Table 4**: Source contributions at Barcelona (BCN) and Montseny (MSY)

	BCN	MSY
	[μg/m^3; **%**]	[μg/m^3; **%**]
Source		
AgedMarine	5.73; **16.9**	1.76; **10.6**
Mineral	4.61; **13.6**	2.70; **16.2**
AmmSulfate	4.67; **13.7**	3.95; **23.7**
AmmNitrate	4.45; **13.1**	1.31; **7.9**
V-Ni	3.32; **9.8**	0.71; **4.3**
Industrial/Metallurgy	0.96; **2.8**	
Traffic	5.14; **15.1**	
Road/work resuspension	4.25; **12.5**	
Aged Organics		3.78; **22.7**
Industrial/Traffic		1.43; **8.6**

798

799

800

801

802

803

804

805

806

807

808

809

810

811

812

813

814

815

816

817 **Table 5**: Mann-Kendall and Multi-exponential trends of source contributions in PM_{10} from PMF at BCN (bold italic) and MSY. Highlighted
818 source contributions at BCN from Mineral, Traffic and Road/work resuspension were excluded from the trend discussion. Type: linear (L),
819 single-exponential (SE), double exponential (DE); **a** (μgm^{-3}) and τ (yr) are the constants and the characteristic times, respectively, of the
820 exponential data fittings; NL (%) = Non-Linearity; TR (%) = Total Reduction; RC (%) = Residual Component. Significance of the trends
821 following the Mann-Kendall test: *** (p-value < 0.001), ** (p-value < 0.01), * (p-value < 0.05), + (p-value < 0.1).

Source	PM_{10} (**BCN**;MSY)		Mann-Kendall fit		Multi-exponential fit					
	Contribution 2004 (μgm^{-3})	Contribution 2014 (μgm^{-3})	Trend (%/yr)	p-value	type	a (μgm^{-3})	τ (yr)	NL (%)	TR (%)	RC (%)
Ammonium sulfate	*10.27*	*3.38*	*-2.49*	*	*DE*	*12.33* *3.82*	*1.65* *105.80*	*45*	*67*	*16*
	6.57	3.07	-2.02	*	DE	4.92 3.05	2.44 85.63	27	51	21
Ammonium nitrate	*6.99*	*1.96*	*-3.74*	***	*SE*	*8.54*	*8.96*	*14*	*67*	*13*
	2.03	0.47	-3.27	**	SE	2.44	8.59	15	69	17
V-Ni bearing	*4.23*	*1.84*	*-3.11*	**	*SE*	*5.66*	*10.59*	*11*	*61*	*19*
	0.79	0.44	-2.96	**	L	1.13	11.94	8	57	25
Industrial/Metallurgy (BCN)	*1.64*	*0.71*	*-3.43*	***	*DE*	*1.89* *0.0015*	*7.41* *-2.06*	*29*	*56*	*11*
Mineral	*4.61*	*3.01*	*-1.87*	+	*L*	*6.53*	*16.19*	*12*	*64*	*46*
	3.46	2.32	-1.71	+	L	3.34	27.46	5	46	34
Marine	*5.67*	*4.91*	*-1.40*		*L*	*6.45*	*47.09*	*1*	*19*	*14*
	1.53	1.89	0.62		L	1.71	-107.83	0	-10	24
Industrial/Traffic (MSY)	2.08	1.01	-3.11	**	L	2.18	12.94	7	54	11
Aged Organics (MSY)	3.14	3.26	1.25		L	3.34	-51.05	1	-22	17
Traffic (BCN)	*8.21*	*3.33*	*-2.65*	**	*SE*	*9.87*	*8.82*	*15*	*68*	*21*
Road/work resuspension (BCN)	*7.33*	*0.89*	*-2.80*	**	*SE*	*10.52*	*6.15*	*27*	*80*	*41*

822

823

824

825

826

827

828

829

830

831

Atmospheric
Chemistry
and Physics
Discussions

Open Access

EGU

832 **Figure Captions:**

833 **Figure 1**: Location of the Barcelona (BCN) and Montseny (MSY) measuring stations. Red full circle highlights the location of the BCN

834 measuring station before 2009. Green full circle highlights the new location of the BCN (from 2009) and MSY measuring stations.

835 **Figure 2**: Mann-Kendall (a) and Multi-exponential (b) fits of $PM_{2.5}$ trends at MSY station for the periods 2002-2010 (as in Cusack et al.,

836 2012), 2004 – 2014 (this work), and 2002 – 2014 (largest period so far available). TZ_MK: Mann-Kendall trend (%/yr); S_MK: significance

837 of Mann-Kendall trend; a_n: multiplicative constant of exponential function ($\mu g/m^3$); τ_n: characteristic time of exponential function (yr);

838 NL: non-linearity (%); TR: total reduction (%); RC: residual component (%).Significance of the trends following the Mann-Kendall test: ***

839 (p-value < 0.001), ** (p-value < 0.01), * (p-value < 0.05), + (p-value < 0.1).

840 **Figure 3**: Mann-Kendall (MK) and Multi-exponential (ME) trends for chemical species at BCN in PM_{10}. Measured concentration (green

841 line); Multi-exponential trend (red line); Multi-exponential residuals (blue line); Mann-Kendall trend (black line); Mann-Kendall residuals

842 (grey line). Trend type: linear (L), single-exponential (SE), double exponential (DE).

843 **Figure 4**: Mann-Kendall (MK) and Multi-exponential (ME) trends for chemical species at MSY in PM_{10}. Measured concentration (green

844 line); Multi-exponential trend (red line); Multi-exponential residuals (blue line); Mann-Kendall trend (black line); Mann-Kendall residuals

845 (grey line). Trend type: linear (L), single-exponential (SE), double exponential (DE).

846 **Figure 5**: Source contributions from PMF model in PM_{10} at Montseny (MSY) and Barcelona (BCN). Mean values during 2004-2014. Values

847 reported are: ***Source; $\mu g/m^3$; %.***

848 **Figure 6:** Mann-Kendall and Multi-exponential trends for source contributions in PM_{10} at BCN. Measured concentration (green line);

849 Multi-exponential trend (red line); Multi-exponential residuals (blue line); Mann-Kendall trend (black line); Mann-Kendall residuals (grey

850 line). Trend type: linear (L), single-exponential (SE), double exponential (DE). Highlighted with yellow colour the source contributions at

851 BCN from *Mineral*, *Traffic* and *Road/work resuspension* were excluded from the trend discussion.

852 **Figure 7**: Mann-Kendall and Multi-exponential trends for source contributions in PM_{10} at MSY. Measured concentration (green line);

853 Multi-exponential trend (red line); Multi-exponential residuals (blue line); Mann-Kendall trend (black line); Mann-Kendall residuals (grey

854 line). Trend type: linear (L), single-exponential (SE), double exponential (DE).

855 **Figure 8**: NASA NO_2 OMI level 3 plotted using the Giovanni online data system, developed and maintained by the NASA GES DISC.
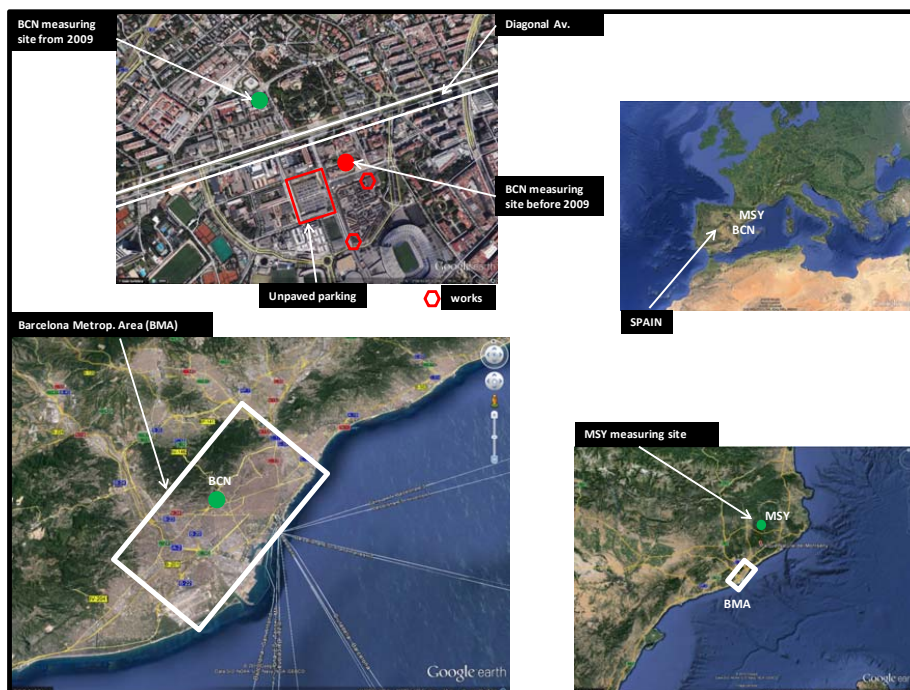
856 **Figure 9**: Annual (2004–2014) energy consumption for Spain (normalized to year 2004). Data from the Spanish Ministry of Industry

857 (MINETUR, 2013).

858 **Figure 10**: Spanish national emission of SO_2 and NO_X (normalized to year 2004).
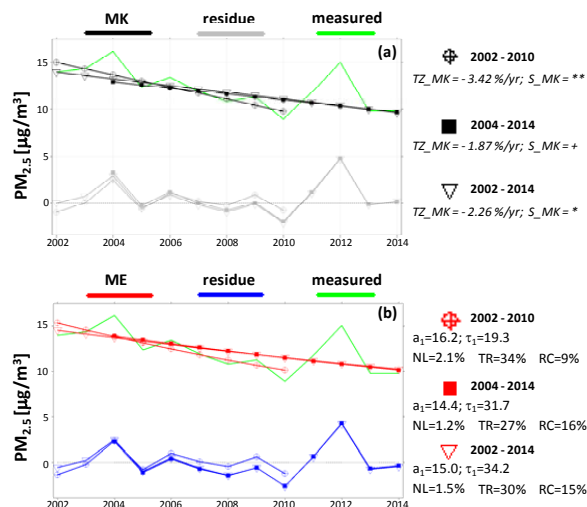
859

860

861

Figure 1

870

871 **Figure 2**

872
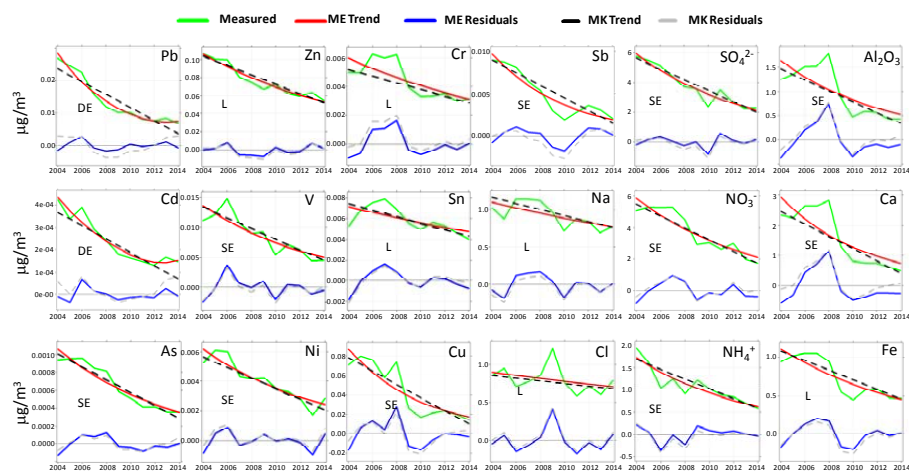
873

874

875

876

877 **Figure 3**

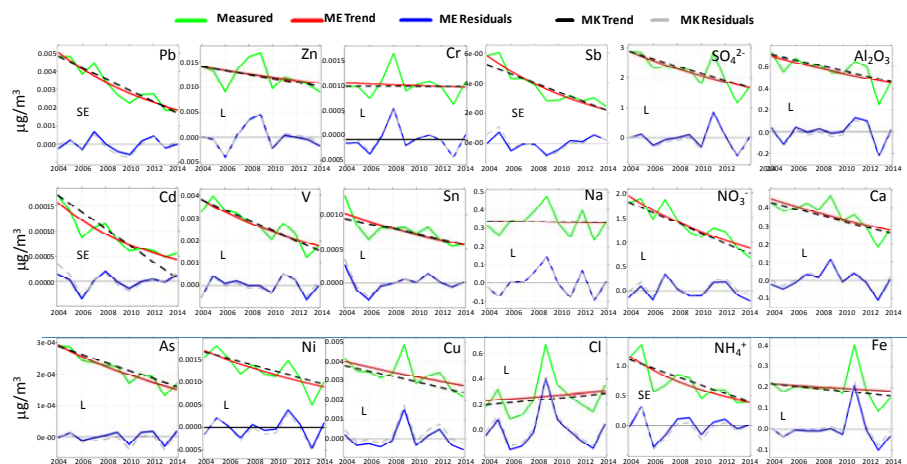878

879

880
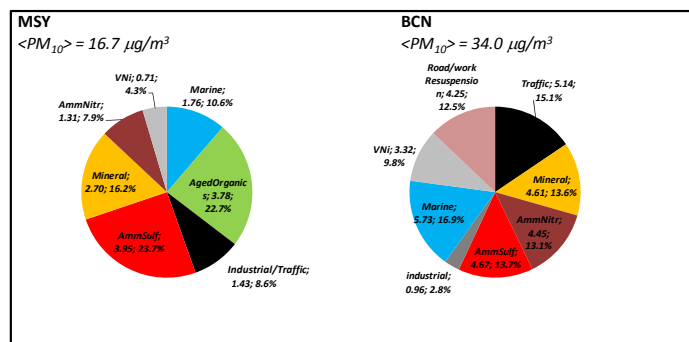
Atmospheric
Chemistry
and Physics
Discussions

881

882

Figure 4

884

885

886

887

Figure 5

889

890

891
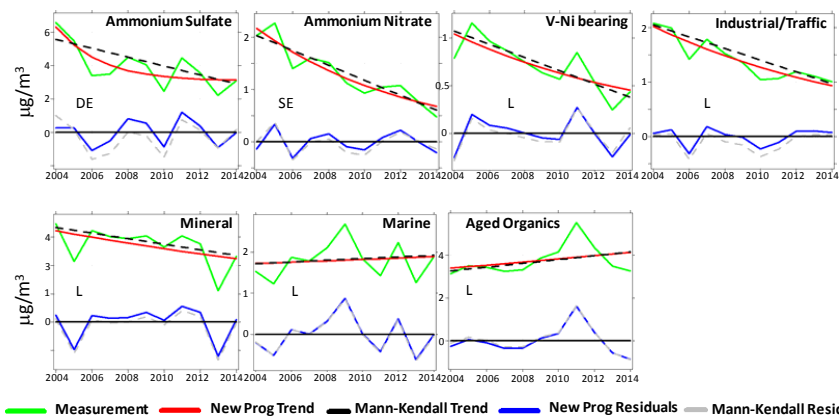
892

893

894

895
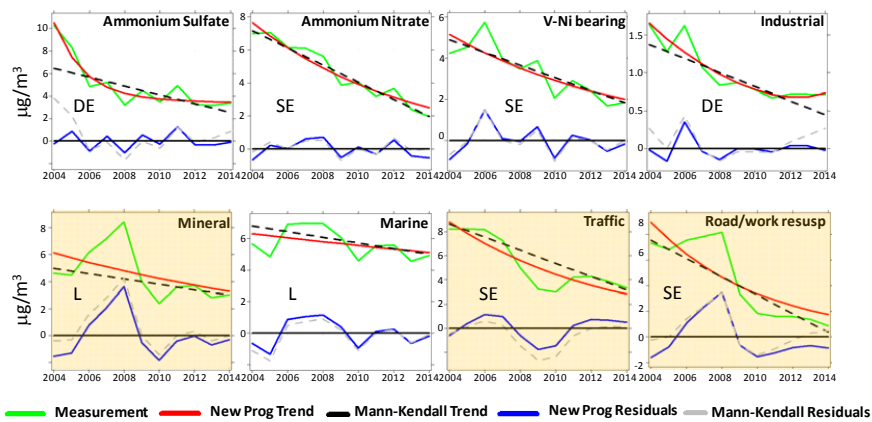
Figure 6

896

897

898

899
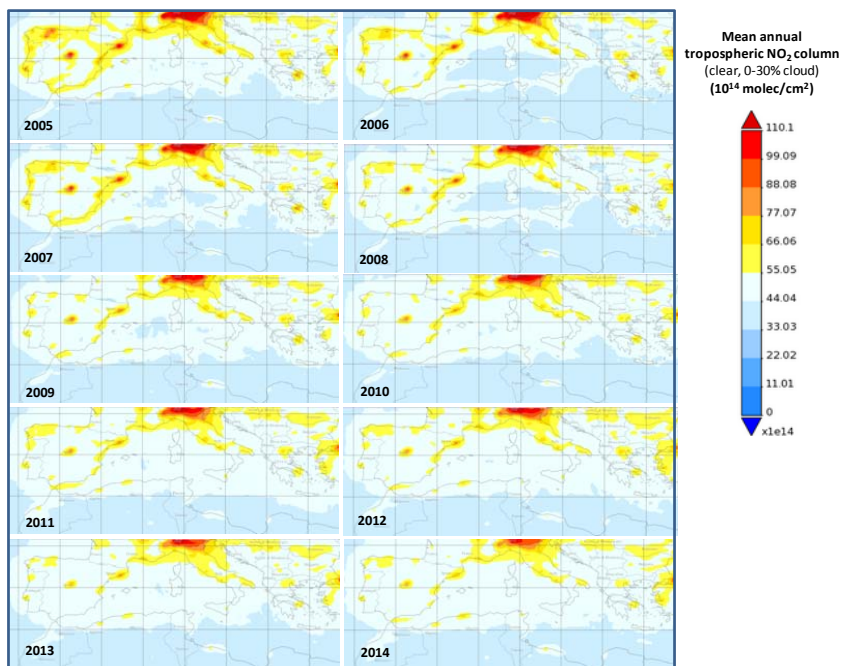
900

901

Figure 7

902

903

904

905

906

907

908

Figure 8

909

910

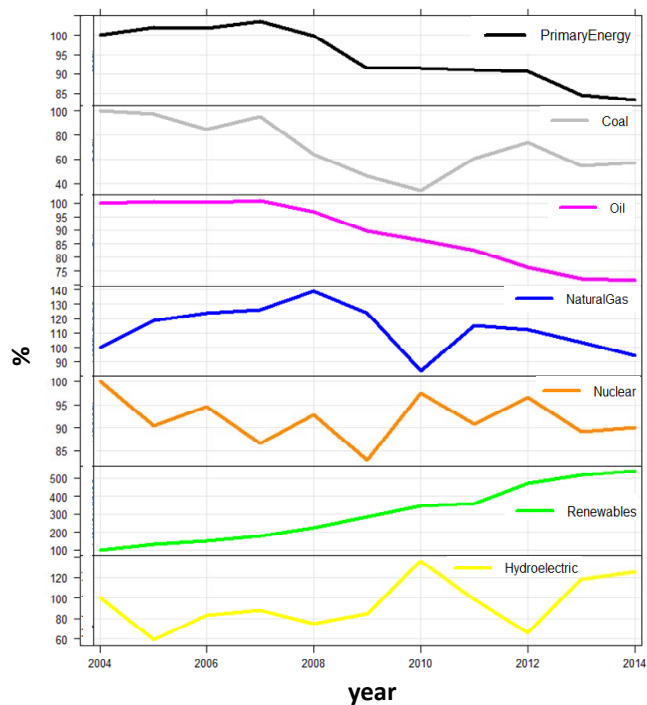911

912
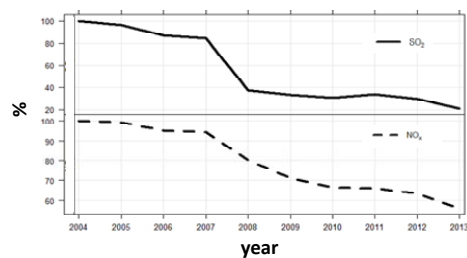
913

914

915

916

917

918

919

920

921

922

923 **Figure 9**

924

925

926

927 **Figure 10**

928

929